Addis Ababa University

Addis Ababa Institute of Technology

School of Electrical and Computer Engineering

Performance Analysis of Spectral Efficiency for 5G Enhanced Mobile Broadband Network with Massive MIMO

By

Kahsay Nguse

A Thesis Submitted to Addis Ababa Institute of Technology in Partial Fulfillment of The Requirements for the Degree of Master of Science in Electrical and Computer Engineering (Communication Engineering)

Advisor: Dr. Eng. Yihenew Wondie

Addis Ababa, Ethiopia

January 21, 2022

Addis Ababa University

Addis Ababa Institute of Technology

School of Electrical and Computer Engineering

Performance Analysis of Spectral Efficiency for 5G Enhanced Mobile Broadband Network with Massive MIMO

By: Kahsay Nguse

Approval by Board of Examiners

______________________	___________	_________
Dean, School of Electrical and Computer Engineering	signature	Date
Dr. Eng. Yihenew Wondie	__________	__________
Advisor	signature	Date
1. _____________________	__________	__________
Internal examiner	signature	Date
2. _____________________	___________	_________
External examiner	signature	Date

Declaration

I, the undersigned, declare that this MSc thesis is my original work, has not been presented for fulfillment of a degree in this or any other University and all sources and materials used for the thesis are duly acknowledged.

Kahsay Nguse Gebrekidan ______________

Name Signature

Addis Ababa ______________

Place Submission date

This thesis work has been submitted for examination with my approval as a university thesis Advisor.

Dr. Eng. Yihenew Wondie ______________

Advisor's Name Signature

Acknowledgments

First of all, I am thankful for the almighty of God for the good health and well-being that has enabled me to complete this work.

I would like to express my sincere gratitude to my advisor Dr. Eng. Yihenew Wondie for his continuous support, patience, motivation, understanding and immense knowledge. His guidance helped me in all the time of research and writing of this thesis.

I am also very grateful to my family, colleagues, friends and others whom positively or negatively contributed in many ways for successful accomplishment of this thesis.

Abstract

Due to the increase of the number of users and applications, the improvement of technology is also ongoing. Wireless mobile communications need high data rate and capacity at the same time. Future generation wireless communication will have to deal with some basic requirements for serving large number users with high throughput. The fifth generation (5G) network needs to evolve in order to increase the capacity higher than the fourth generation of networks by 2025.

In practice, the inter-user interference in multi-cell network has impact when more users access the wireless network and reduces performance of the system. This thesis explains the basic motivations behind Massive MIMO technology in application to 5G enhanced mobile broadband network, and provides analysis for spectral efficiency in different propagation environments. First, Lower bound SE expressions are derived to enable efficient system-level analysis under LoS and NLoS propagation environments under the assumption that channel state information is acquired by using pilot sequences (reused across the network) with densification of BSs so as to improve the SE for UEs.

Simulations are used to show what happens to SE for different path loss models, BS antennas M, and different UEs K under these propagation environments. The numerical analysis shows that the SE as a function of BS density achieves its maximum for a relatively small density of BS, irrespective of the processing scheme used. This is different from distance-independent path loss model, in which the SE is a non-decreasing function of BS density. ZF processing is found to be good compensation in complexity and performance in spectral efficiency, which is then used to optimize, for a given BS density, the pilot reuse factor, number of BS antennas and UEs.

Keywords*: Massive MIMO system, eMBB, LoS and NLoS propagation, Distance dependent path loss, Area Spectral efficiency, and optimal power control schemes.*

Table of Contents

List of Figures

List of Tables

List of Symbols

h	scalar h
$\mathbf{h}$	Vector h
H	matrix H
$\mathbb{R}$	Set of real numbers
$\mathbb{C}$	Set of complex numbers
f	frequency reuse factor
s	coherence block length
$(.)^*$	Complex conjugate
$(.)^T$	Transpose of matrix
$(.)^{-1}$	Inverse of matrix
$\mathrm{E}[.]$	Mean of the random variable
$\|.\|$	Norm of vector
$\lvert . \rvert$	Absolute value

List of Abbreviations

3GPP	Third Generation partnership project
BW	Bandwidth
DL	downlink
UL	Uplink
MIMO	Multiple input multiple output
MU-MIMO	Multi user multiple input multiple output
eMBB	Enhanced mobile broad band network
NR	New radio
CSI	Channel state information
i.i.d	independent and identically distributed
LTE	long term evolution
TDD	Time division duplexing
ZF	Zero force
MRT	Maximum ratio transmission
M-MMSE	Multi-cell minimum mean square error
SDMA	Space division multiple access
UE	User ends
BS	Base station
SE	Spectral efficiency
CDF	Cumulative distribution function
ITU	International telecommunication union

Chapter 1
Motivation and Background

1.1 Introduction

Now a days, the number of users and devices need to connect to a network are increasing from time to time leading to a demand of huge amount of data and bandwidth. The next generation network (5G) is expected to provide capacity to handle growing data traffic, number of connected devices, as well as present opportunities for operators to grow and improve their consumer business. 5G goes beyond improved quality network performance and speed, providing new and improved connected access points for users. 5G, however, takes it to the next level, introducing the concept of massive MIMO, which as the name implies involves the application of MIMO technology on a much larger scale for greater network coverage and capacity. 5G is expected to be the most flexible way to gain benefit from all available spectrum alternatives, including licensed, shared access and unlicensed, and TDD. 5G differs from previous generations in that it is expected to integrate different mobile technologies, rather than simply replacing previous generations. For this reason 5G is sometimes referred to as a network of networks or a system of systems, with a potential to encompass a variety of technologies and access models [7, 8].

As shows in figure (1.1) the mobile data and traffic and the number of connected devices increase fast from time to time, particularly, from 2017-2022. This huge amount of mobile data traffic is challenging to manage with the capabilities of previous wireless generation systems.

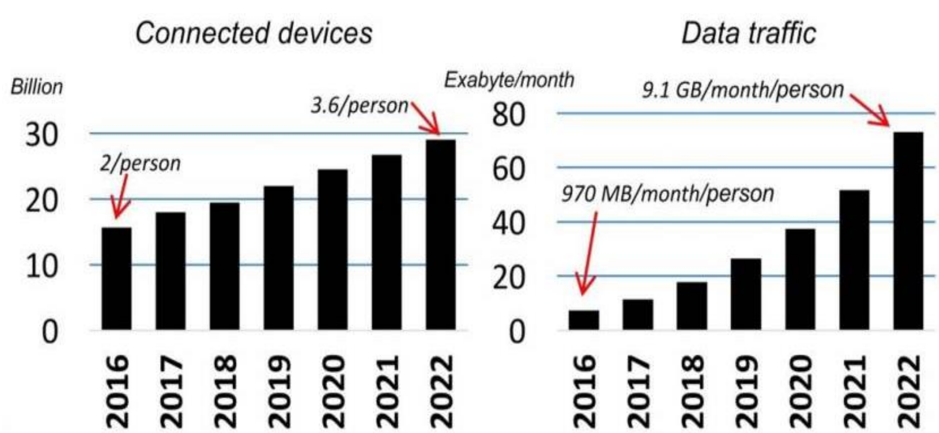

Figure 1.1: Global mobile data traffic and growth in connected devices from 2016 to 2022 [8].

As in figure (1.2), the key usage scenarios identified by ITU, in which 5G is expected to support, and provide service are:

- ✓ **Enhanced Mobile Broadband (eMBB) Service: -** This is the first stage of 5G adoption and is expected to provide high bandwidth services for wireless connectivity. 5G enhanced mobile broadband (eMBB) focuses on supporting the ever-increasing end user spectral efficiency, data rate and system capacity. To fulfill this demand, eMBB introduces two major technology enhancement techniques:
  - Antenna array that includes tens or even hundreds of Tx/Rx antenna elements to enable massive MIMO and beamforming which is used in this thesis work.
  - Shift of frequency spectrum to cmWave and mmWave range to achieve much higher bandwidth allocation.

To do so, 5G will cover a broad range of use cases, which lay within the spectrum of different use cases. It aims to improve consumer experience when accessing multimedia content, services and data and focuses mainly on services with high bandwidth requirements.

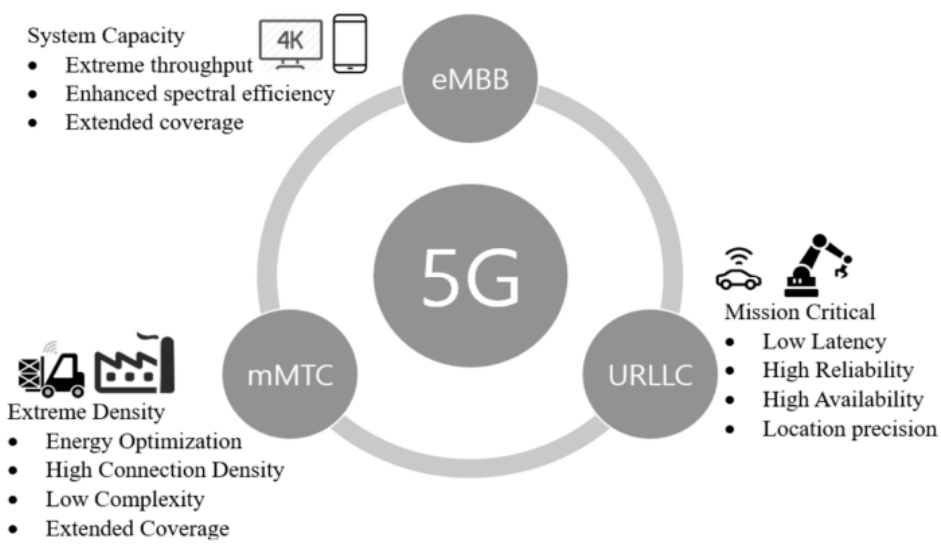

Figure 1.2: Application of 5G Massive MIMO System

Massive MIMO in application to 5G is expected to provide multiple increase of in data rates, serves and supports ten to hundred times higher than the number of access points or devices. The performance of any cellular network is obstructed at the physical layer, because, the amount of information that can be transferred between the receiver and transmitter is limited by the availability of spectrum, the laws of electromagnetic propagation properties, propagation environments and effects, and the concepts of information theory and coding techniques. The basic different techniques in which efficiency of a wireless system may be improved:

- Densification of BSs and access points;
- More spectrum usage; and
- Improving the spectral efficiency, which is, the number of bits that can be conveyed per second in each unit of bandwidth. While future cellular networks and principles are likely to use an ever-increasing density and use new spectral bands, for the need of improving spectral efficiency in a given band never vanish.

The first concept in the ongoing improvement of cellular system is that it is dependent in either increasing bandwidth or increasing the density of small cells to achieve the required area throughput. The third factor is the one which can improve area throughput that implies spectral efficiency, and has remained almost unchanged during the rapid network development and growth of the cellular system. Efficient cellular network technology which increases the area throughput without increasing the bandwidth of the cell is essential to achieve the fast growing data traffic demands faced by the wireless carriers [15, 16].

1.2. Literature Review

To enforce efficiency and maintain a reliable communication in 5G network using Massive MIMO system, a lot of researches have been done which most of them have mainly focused on the Massive MIMO system and precoding techniques. Massive MIMO concept, which has been identified as the key technique to increase the Spectral efficiency (SE) over contemporary systems has focused in single-cell and multi-cell networks [4, 5]. Some of the reviewed related works on Massive MIMO spectral efficiency systems are given as follows:

Jehangir Arshad, Abdul Rahman, Ateeq Ur Rehman, Rehmat Ullah and Seong Oun Hwang [2020], in this paper SE is analyzed for the next generation network. They derived the deterministic channel model and evaluated the spectral efficiency. The simulation result validates the proposed channel model in real time. The finding shows that the SE is substantiate using uniform linear array configuration [7].

Antonio Rouxinol Fragoso, Antonio Rodrigues, and Diogo X. Almeida*y*, Instituto Superior Tecnico, Vodafone Portugal, the authors implemented the impact of Massive MIMO antenna on high capacity 5G-NR networks under different configurations. They found that one antenna serving the whole area in hotspot based configurations gives the best performance [8].

Felipe A. P. de Figueiredo, Fabbryccio A. C. M. Cardoso*y*, and Gustavo Fraidenraich, Ghent University, IT, Ghent, Belgium, authors in this paper evaluates the feasibility of Massive MIMO in tackling the Uplink mixed service of communication problem under the assumption of available physical narrow band shared channel. The finding shows that the proposed MSE estimator result asymptotically approaches to the MMSE. They also derived the closed- form MMSE expressions for MSE.

Amin Ghazanfari, [2019], in this work the author analyzed different optimal Power Control algorithms for Multi-Cell Massive MIMO system. The sum SE is investigated and analyzed for different system parameters. The optimization problem for the power control schemes is solved using geometric optimization and sum SE is maximized and improved with proportional fairness better than max-min fairness scheme [22].

Ali M A and E. A. Jasmin [2017], worked on the optimization of spectral efficiency (SE) of Massive MIMO in time division duplex (TDD) architecture. The SE performance is compared under different linear precoding techniques like, zero forcing (ZF) and maximum ratio precoding (MRT). Numerical results show that massive MIMO with hundreds of BS antennas can easily improve spectral efficiency. Optimization TDD Massive MIMO architecture using MRT and ZR processing in multi-cell networks under different system parameters [18].

Hoon Huh, Giuseppe Caire and Haralabos, [2011], this work analyzed closed-form based large system limit in all dimension to scale up to infinity values with fixed ration. This makes use of latest works on the analysis of cellular networks with linear zero-forcing beamforming and channel estimation errors.

Efficiency improvement of cellular networks has received great attention in the literature of wireless networks. The first attempts were based on the simple Wyner model [35] wherein both BSs and UEs are located on a line at fixed positions. Within the stochastic geometry framework, the locations of BSs form a point process in a compact set whose cardinality is a Poisson distributed random variable that is independent among different disjoint sets. The performance of a cellular network can be measured in many different ways such as coverage probability, throughput, and SE. many researches consider the standard path loss model where received power decays over a distance. But in this work distance dependent path loss model is used and analyzed where densification pushes many BSs to the near field.

1.3 Statement of the problem

The major challenges in wireless network include spectral efficiency, coverage and energy efficiency. This is due to the limited available bandwidth, the fading nature of the propagation channel and the mobility and autonomy of wireless nodes. The rapid growth in demand for high speed and high quality mobile and data services with diverse quality of service requirement is also creating the opportunities and challenges for wireless system designers. Researches over the last decades focused towards improving spectral efficiency, so that higher data rates can be achieved within a given bandwidth. The motivation behind Massive MIMO system is, that with the increase of antennas in a BS antennas with in a cell the random channel vectors between the users and base station become nearly orthogonal, it reduces the transmitted power; in the uplink, reducing the power of the terminals will save their battery life where as in the downlink, much of the electrical base station power is spent by power amplifiers and associated circuits and cooling systems. This study explores massive MIMO system in 5G eMBB network. Zero Forcing, Maximum Ratio, and Multi-cell minimum mean squared error are used as main processing techniques.

1.4. Objective of the thesis

The following general and specific objectives are to be accomplished in this thesis.

1.4.1. General Objective

The General objective of the thesis is to analyze spectral efficiency in 5G Enhanced Mobile Broadband using Massive MIMO System.

1.4.2 Specific Objectives To:

- ✓ Review the basic concept of Massive MIMO wireless network.
- ✓ Study Massive MIMO in eMBB services
- ✓ Derive SE under LOS and NLOS propagation environments
- ✓ Analyze SE in distance dependent path loss model
- ✓ Optimize and maximize SE using power control techniques

1.5 Methodology: The formal methodologies followed to achieve the objectives of this thesis work are:

- **Literature review**: includes reading books, articles, simulation tools and other resources related to signal processing techniques, channel estimation algorithm, Massive MIMO, cellular network, Spectral efficiency, throughput, power control algorithms and other related papers.
- **System modeling and simulation**: includes mathematical modeling of Multi-cell Massive MIMO wireless networks with pilot reuse factor, simple processing techniques and simulating the models using MATLAB.
- **Performance comparison**: this includes the performance comparison of simple processing techniques for different number of users, BS antennas, pilot reuse factor, and Spectral-efficiency in Rayleigh fading channel.
- **Result and conclusion**: the results obtained from the implemented system is studied.
- **Recommendation**: at the end a recommendation for the feature research work will be given.

1.6. Thesis Contribution and Organization

In the literatures discussed so far in Section (1.2), but some of the differences in the previous work and the current work are discussed here.

Base Stations are independently and uniformly distributed in a given geographical area according to intensity of D. Channel inversion power-control is employed in the uplink (UL) to achieve a uniform average signal-to-noise ratio (SNR) across all the UEs. The UL channel is estimated and used then in the DL case due to the principle called channel reciprocity.

The basic contributions of the thesis are:

- Study different 5G services like, enhanced mobile broadband network which is one of the specific application of Massive MIMO System
- We see that the potential research directions and applications of 5G services for mobile operators.
- Derived lower bound and closed form SE expressions in LoS and NLoS propagation environments considering inter-cell and intra-cell interference.

- The SE of the network is computed by using a lower bound on the average spectral efficiency which is valid for any processing schemes in distance dependent path loss model.

This thesis is organized into five chapters. The first Chapter deals about the proposal for implementation of Massive MIMO in 5G enhanced Mobile broadband network, the second Chapter deals about the overview of Massive MIMO System, Chapter three deals about SE under LoS and NLoS channel models with distance dependent path loss model using simple processing techniques. The fourth Chapter deals about system analysis, simulation results and discussion found from Chapter three and finally Chapter five draws a conclusion and recommendation about the research outcome and future directions.

Chapter 2

Massive MIMO System

2.1 Introduction

Spatial multiplexing gain has transferred from MIMO to multiuser MIMO, where UEs are simultaneously served by a multiple-antenna base station (BS). MU-MIMO simply overcomes most of propagation limitations in MIMO such as distorted and polluted channels. Line-of-sight propagation, which causes significant reduction of the performance of MIMO systems, is no longer a problem in MU-MIMO systems.

Thus, MU-MIMO has attracted substantial interest. There are three fundamental distinctions between Massive MIMO and conventional Multiuser MIMO [16, 19].

i. Only the base station learns G.
ii. M is typically much larger than K, although this does not have to be the case.
iii. Simple linear signal processing is used both on the uplink and on the downlink.

Figure (2.4) shows the basic setup for Massive MIMO where, each base station with number of antennas M serves a cell with a large Number of UEs, K. Different base stations serve different cells, and is assumed that there is no cooperation among base stations.

Let

$$H_{l'}^{l} = \left[h_{l',1}^{l} \ldots h_{l',K}^{l} \right] \in \mathbb{C}^{MxK} \tag{2.1}$$

Be the MxK channel matrix between an M-antenna at the l^{th} base station and K-user terminals that are served by the l' base station. Common number of BS antennas and number of UEs are assumed in each cell. The antennas at each base station work coherently together, but different base stations do not cooperate. the same carrier frequency is used in all particular cells, and inter-cell interference then results.

2.2 Uplink Massive MIMO System

The signal received at the m^{th} base station antenna in the l^{th} cell denoted by y_{lm}, is a superposing of signals transmitted from the K terminals in the l^{th} cell, and the $K(\mathrm{L}-1)$ terminals in all interfering cells $l' = 1, \ldots, l-1, l-1, l+1, \ldots, L.$ mathematically, this can be shown as;

$$y_{\mathrm{lm}} = \sqrt{\rho_{ul}} \sum_{k=1}^{K} h_{lk}^{lm} x_{lk} + \sqrt{\rho_{ul}} \sum_{\substack{l'=1 \\ l' \neq l}}^{L} \sum_{k=1}^{K} h_{l'k}^{lm} x_{l'k} + w_{lk}, \tag{2.2}$$

Where $x_{l'k}$ is the signal transmitted by the k^{th} terminal in the l' cell and $h_{l'k}^{lm}$ is the channel gain from the k^{th} terminal in the l'^{th} cell to the m^{th} base station antenna in the l^{th} cell ; as shown in figure (2.1). The last term in (2.2) is the additive receiver noise, which we assume is CN (0, 1) and independent among different m and l. in vector form,

$$y_l = \sqrt{\rho_{ul}} H_l^l x_l + \sqrt{\rho_{ul}} \sum_{\substack{l'=1 \\ l' \neq l}}^{L} H_{l'}^l x_{l'} + w_l, \tag{2.3}$$

Where $y_l = \left[y_{l1}, \ldots, y_{lm} \right]^T$, $w_l = \left[w_{l1}, \ldots, w_{lm} \right]^T$,

$$H_l^l = \begin{bmatrix} h_{l1}^{l1} & \cdots & h_{lK}^{l1} \\ \vdots & \ddots & \vdots \\ h_{l1}^{lM} & \cdots & h_{lK}^{lM} \end{bmatrix} \tag{2.4}$$

Is MxK matrix that contains all channel gains from the terminals in the $l'th$ cell to the base station array in the l^{th} cell and the K-vector $x_{l'} = \left[x_{l'1}, \ldots, x_{l'\mathrm{K}} \right]^T$ contains the signals transmitted by the terminals in the l^{th} cell.

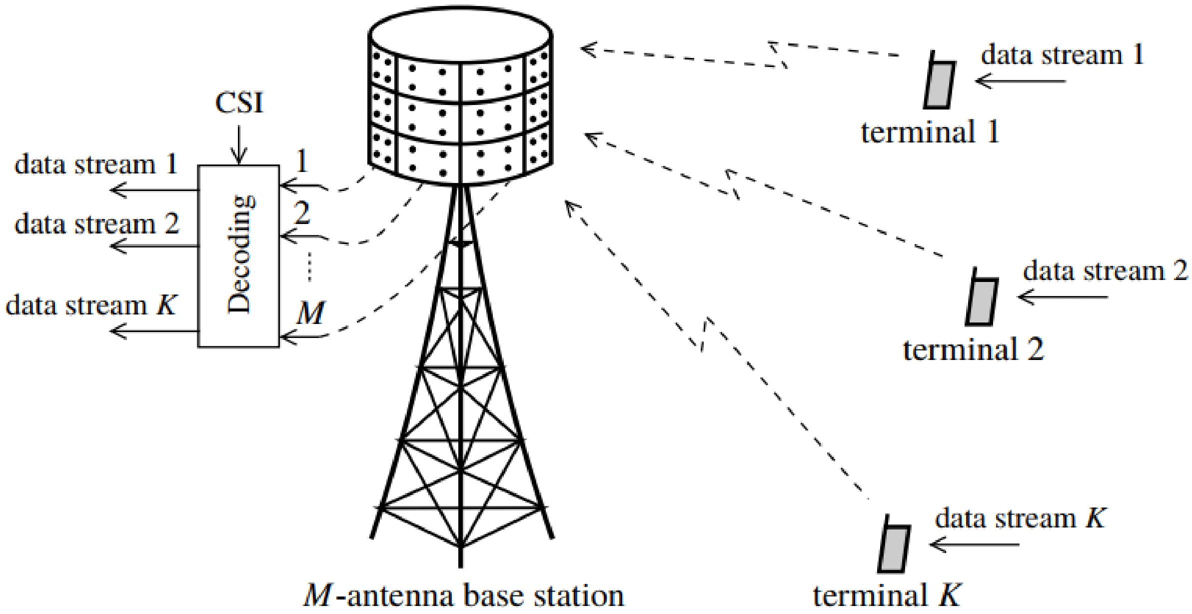

Figure 2.1: Uplink Massive MIMO System

2.3 Downlink Massive MIMO System

In the downlink under the assumption of reciprocity, the k^{th} terminal in the l^{th} cell receives

$$y_{lk} = h_{lk}^{lT} x_l + \sqrt{\rho_{dl}} \sum_{\substack{l'=1 \\ l' \neq l}}^{L} h_{lk}^{l'T} x_{l'} + w_{lk} \tag{2.5}$$

Where $h_{lk}^{l'}$ is the k^{th} column of $H_l^{l'}$, $x_{l'}$ represents the M-vector transmitted by the array in the l^{th} cell, and w_{lk} is noise with distribution $CN(0,1)$. Collectively, the K terminals in the l^{th} cell will receive the K-vector

$$y_l = \sqrt{\rho_{dl}} H_l^{lT} x_l + \sqrt{\rho_{dl}} \sum_{\substack{l'=1 \\ l' \neq l}}^{L} H_l^{l'T} x_{l'} + w_l \tag{2.6}$$

Where $y_l = [y_{l1}, ..., y_{lK}]^T$ and $w_l = [w_{l1}, ..., w_{lK}]^T$ is a K vector of noise with i.i.d CN (0, 1).

The BS has to ensure that each UE receives the intended signal in the DL. The multiplexing and de-multiplexing signal processing is made possible by utilizing a large number of antennas and by its possession of CSI at the BS.

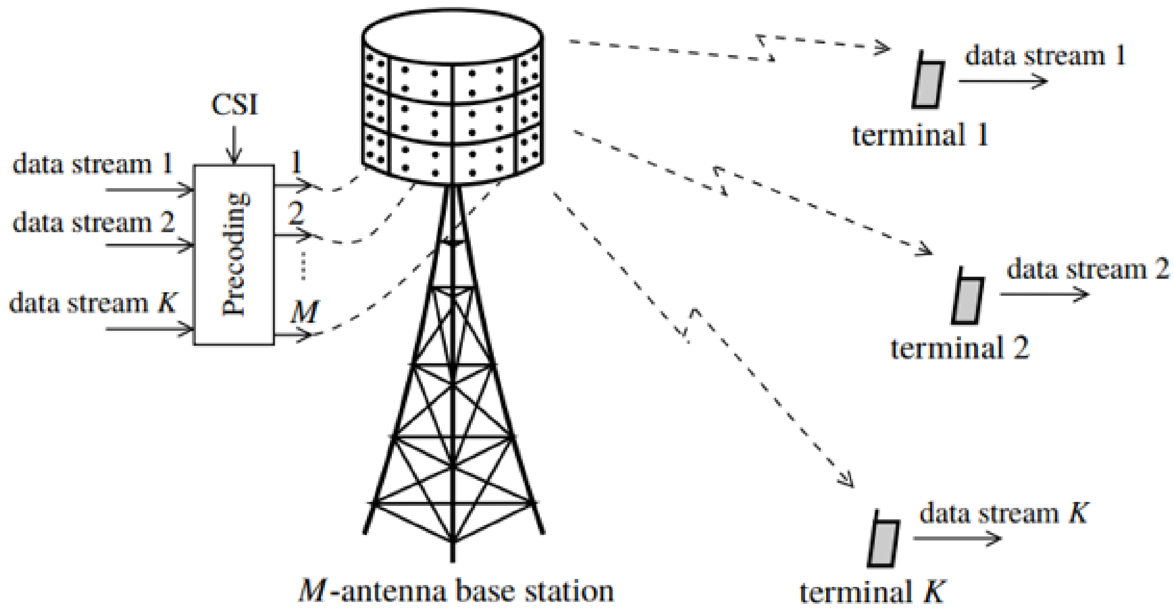

Figure 2.2: Downlink Massive MIMO System

As illustrated in figure (2.3(a)), under LoS propagation conditions, the base station creates, for each terminal, a beam within a narrow angular window centered on the direction to the terminal.

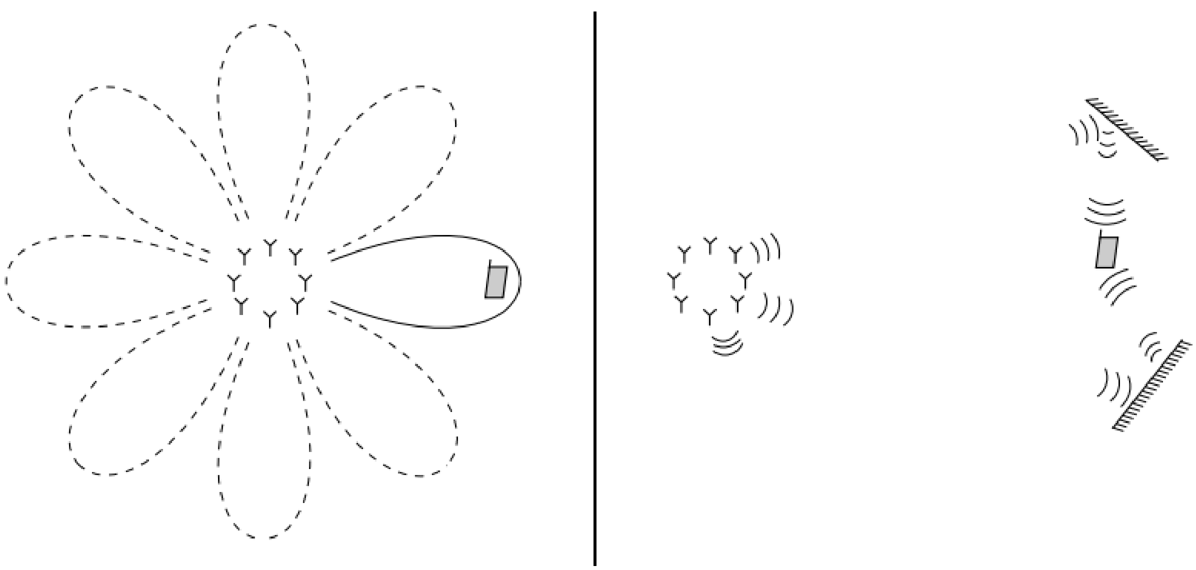

(a) LOS propagation (b) Propagation environment with scattering

Figure 2.3: Effects pf precoding in different propagation environments [16]

When more antennas are used the beam becomes narrow and forces the signal direction towards the desired user. Transmitted waveforms must be chosen properly to superimpose different signal components constructively; as in figure 2.3(b), the more antennas, accurate CSI at the BS is essential.

In [15], Marzetta showed that the use of large number of BS antennas compared to the number of UEs makes linear processing nearly optimal. due to the use of large number of antennas at the Massive MIMO BSs, the effect of small-scale fading of wireless propagation channels are averaged out and this is called favorable propagation, assume the pair of channels h_{lk}^{l} and $\hat{h}_{lk}^{l}$ to BS j provide asymptotically favorable propagation if

$$\frac{\left(h_{lk}^{l}\right)^{T}\hat{h}_{lk}^{l}}{\sqrt{\mathrm{E}\left\{\left\|h_{lk}^{l}\right\|^{2}\right\}\mathrm{E}\left\{\left\|\hat{h}_{lk}^{l}\right\|^{2}\right\}}}\rightarrow 0 \tag{2.7}$$

Almost surely as $M \rightarrow \infty$. This equation says that the inner product of the normalized channels

$$\frac{h_{lk}^{l}}{\sqrt{\left\{\mathrm{E}\left\|h_{lk}^{l}\right\|^{2}\right\}}} \text{ And } \frac{h_{lk}^{l}}{\sqrt{\mathrm{E}\left\{\left\|h_{lk}^{l}\right\|^{2}\right\}}} \tag{2.8}$$

Goes asymptotically to zero. Since the norms of the channels grow with M_j, favorable propagation does not imply that the inner product of h_{lk}^{l} and h_{lk}^{l} goes to zero; i.e., the channel directions become orthogonal, but not the channel responses. When the channel is less susceptible to the small-scale fading effects and behaves more like a deterministic when we are using all the antennas is called channel hardening. This property alleviates the need for combating small-scale fading. It is clear that LoS channels provides channel hardening.

In NLOS propagation

$$\frac{\left\|h_{lk}^{l}\right\|^{2}}{\mathrm{E}\left\{\left\|h_{lk}^{l}\right\|\right\}}\rightarrow 1 \tag{2.9}$$

$$\frac{\left\|h_{l'}^{l}\right\|^{2}}{\mathrm{E}\left\{\left\|h_{l'}^{l}\right\|^{2}\right\}}=\frac{\left\|h_{l'}^{l}\right\|}{M\beta_{l'}^{l}}\rightarrow 1 \tag{2.10}$$

Almost surely as $M \rightarrow \infty$. This definition says that $\left\|h_{lk}^{l}\right\|^{2}$ of an arbitrary fading channel h_{lk}^{l} is close to its mean value when there are many antennas.

2.5 Uplink Received Signal Model

The uplink system is a link in which a UE sends signal to a BSs in a given cell. We call $x_{li} \sim N_{\mathbb{C}}\left(0, \mathrm{p}_{li}\right)$ the UL payload data signal transmitted from UE i of cell l to its serving BS l with power $p_{li}=\mathrm{E}_{x}\left\{\left|x_{li}\right|^{2}\right\}$. the signal $y_{j} \in \mathbb{C}^{M}$ received at the BS j is

$$y_{j}=h_{jk}^{j} x_{jk}+\sum_{\substack{i=1 \\ i \neq k}}^{K} h_{ji}^{j} x_{ji}+\sum_{l \in \Phi_{D} \backslash\{j\}} \sum_{i=1}^{K} h_{li}^{j} x_{li}+n_{j} \tag{2.11}$$

The first part is the desired signal, the second intra-cell interference, the third is inter-cell interference and the last with $n_{j} \sim N_{\mathbb{C}}\left(0, \sigma^{2} I_{M}\right)$ is the additive Gaussian noise, $h_{li}^{j} \in \mathbb{C}^{M}$ is the channel response between UE i and cell l and BS j modeled as $h_{j}^{li} \sim N_{\mathbb{C}}\left(0, \beta_{li}^{j} I_{M}\right)$, where β_{li}^{j} is the large scale fading coefficient. Since this model considers distance dependent path loss model, we call d_{li}^{j} the distance of UE i in cell l from BS j and compute β_{li}^{j} according to a general distance dependent path loss model, which is given by:

$$\beta_{li}^{j}=\gamma_{n}\left(d_{li}^{j}\right)^{-\alpha_{n}} \tag{2.12}$$

With $\left(d_{li}^{j}\right)$ in [km], for $n=1,\ldots N$. The coefficients $\left\{\gamma_{n}\right\}$ and $\left\{\alpha_{n}\right\}$ are design parameters. Setting N=1 yields the widely used distance independent path loss model which is given by

$$\beta_{li}^{j}=\gamma_{l}\left(d_{li}^{j}\right)^{-\alpha_{1}} \tag{2.13}$$

2.6 Pilot reuse factor and channel estimation

A pilot book $\Phi \in \mathbb{C}^{\tau_p x \tau_p}$ of τ_p mutually orthogonal UL sequences is assumed and used for channel estimation in the UL system. We assume $\phi_{jk} \in \mathbb{C}^{\tau_p}$ as the pilot sequence assigned to the typical user end in cell j . It is also assumed to have normalized UL pilot sequences, to obtain a constant power level, and this implies that $\|\phi_{lk}\|^2 = 1.$ since $\tau_p = fK$, we have considered that the reuse factor is given as

$$f = \frac{\tau_p}{K} > 1$$

In other words there are on average $\mathrm{E}\{\Phi_D\}/\mathrm{f}$ number of cells in the network that share the same pilot network subset. This is modelled in each cell through a Bernoulli stochastic variable which is given by

$$a_{l'l} \sim B(1/f) \text{ For } l' \neq l \text{ and } a_{ll} = 1.$$

Specifically if $a_{l'l} = 1$ all the UEs in cell l' use the same pilot sub set of those in cell l and that causes pilot contamination. We assume as

$$Y_j^p \in \mathbb{C}^{Mx\tau_p}$$

The signal received at BS j during pilot transmission. The vector

$$y_{jli}^p = Y_j^p \phi_{li}^*$$

Obtained by correlating Y_j^p and ϕ_{li} takes the form

$$y_{jli}^p = \sqrt{\rho}\sqrt{p_{li}}h_{li}^j + \sum_{l' \in \Phi_D \setminus \{l\}} a_{l'l}\sqrt{\rho}\sqrt{p_{l'i}}h_{l'i}^j + N_j^p \phi_{li}^* \tag{2.14}$$

Where the first part is the desired pilot, the second the interfering pilots and the third is the noise with $N_j^p \phi_{li}^* \sim N_c(0, \sigma^2 I_M)$ and the power of the UL transmitted payload data is scaled by a factor $\rho = P_p / p_0 \geq 1$ to compensate for the lack of beamforming gain during channel acquisition.

By using $p_{li} = p_p / \beta_{li}^j$, the MMSE channel estimate of h_{li}^j at BS j based on y_{jli}^p is given by

$$\hat{h}_{li}^{j} = \frac{\beta_{li}^{j} / \sqrt{\beta_{li}^{j} p_p}}{\beta_{li}^{j} / \beta_{li}^{l} + \sum_{l' \in \Phi_D \setminus \{l\}} a_{l'l} \, \beta_{l'i}^{j} / \beta_{l'i}^{j'} + 1/SNR} y_{jli}^{p} \tag{2.15}$$

The MMSE estimate $\hat{h}_{li}^{j}$ and error $\tilde{h}_{li}^{j}$, conditioned on a realization of $a_{l'l}$ for all l', $l \in \Phi_D$, are independent and distributed as $\hat{h}_{li}^{j} \sim N_{\mathbb{C}}\left(0, \gamma_{li}^{j} I_M\right)$ and $\tilde{h}_{li}^{j} \sim N_{\mathbb{C}}\left(0, \left(\beta_{li}^{j} - \gamma_{li}^{j}\right) I_M\right)$ where;

$$\gamma_{li}^{j} = \frac{\beta_{li}^{j}}{\frac{\beta_{li}^{j}}{\beta_{li}^{j}} + \sum_{l' \in \Phi_D \setminus \{l\}} a_{l'l} \frac{\beta_{l'i}^{j}}{\beta_{l'i}^{l'}} + \frac{1}{SNR}} \frac{\beta_{li}^{j}}{\beta_{li}^{l}} \tag{2.16}$$

For notational convenience, we define the collecting of all estimates in (4) from all UEs in cell l to BS j as $\hat{H}_l^{j} = \left[\hat{h}_{l1}^{j} \ldots \hat{\mathrm{h}}_{lK}^{j}\right] \in \mathbb{C}^{MxK}$. Note that the estimate $\hat{h}_{li}^{j}$ of a UE I in cell l' using the same pilot sequence of UE i in cell l $\left(i.e. a_{l'l} = 1\right)$ can be obtained from $\hat{h}_{li}^{j}$ in (2.16) as

$$\hat{h}_{l'i}^{j} = \sqrt{\frac{\beta_{li}^{l}}{\beta_{l'i}^{l'}}} \frac{\beta_{l'i}^{j}}{\beta_{li}^{j}} \hat{h}_{li}^{j} \tag{2.17}$$

Where $\hat{h}_{l'i}^{j} \sim N_{\mathbb{C}}\left(0, \gamma_{l'i}^{j} I_M\right)$ has variance

$$\gamma_{l'i}^{j} = \frac{\beta_{li}^{l}}{\beta_{l'i}^{l'}} \left(\frac{\beta_{l'i}^{j}}{\beta_{li}^{j}}\right)^2 \gamma_{li}^{j} \tag{2.18}$$

And estimation error $\tilde{h}_{l'i}^{j} \sim N_{\mathbb{C}}\left(0, \left(\beta_{l'i}^{j} - \gamma_{l'i}^{j}\right) I_M\right)$.

The link is assumed to be reciprocal due to the principle called TDD which refers to separating the uplink and downlink transmissions in the time-domain while using the whole bandwidth; assuming that both happen in the same coherence time. Therefore, in TDD Massive MIMO systems, we require *K* pilot sequences only [19]. Hence, channel estimation does not depend on *M*.

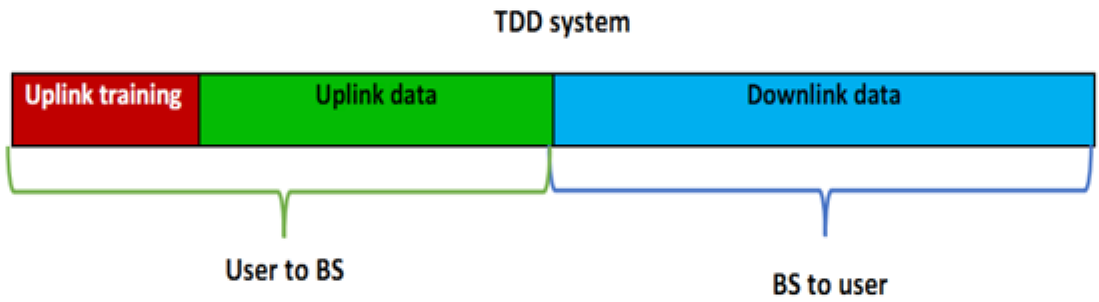

Figure 2.4: Massive MIMO TDD operation

Since the BS uses linear processing schemes to beamform the signals to the users, the user needs only the effective channel gain (which is a scalar constant) to detect its desired signals. Therefore, the BS can spend a short time to beamform pilots in the downlink for CSI acquisition at the users. More precisely, the K users send K orthogonal pilot sequences to the BS on the uplink. Then the BS estimates the channels based on the received pilot signals [20].

Chapter 3

5G Enhanced Mobile Broadband Network

3.1 Introduction

5G Enhanced mobile broad band service focuses on a higher data rate, with a large payload and prolonged internet connectivity based applications. Fixed wireless access for homes and enhanced mobile broadband services are likely to be the first applications using 5G new wireless access modems. The key performance indicators of 5G eMBB network are spectral efficiency, data rate, area traffic efficiency and network energy efficiency. The peak spectral efficiency is 30 bps/Hz and three times more spectral efficiency compared to IMT advanced without increasing energy consumption. 5G networks can support a million devices per square kilometer versus multiple devices in a similar footprint for 4G. Still, for mobile devices, it means that firmware upgrades can deliver new functionality that historically required new and additional hardware [12].

SE in fading channels, which change over time, can be interpreted as the average number of bit/s/Hz over the fading realizations. Furthermore, research and development efforts will continue for even faster speeds, with frequencies approaching hundreds of GHz and beyond. From an electronics design perspective, this is a large chunk of the spectrum with very different signal characteristics between the lower and upper limits of the 5G frequency range. The increased speeds do come with a tradeoffs. Since the propagation environment of the frequencies is very much line of sight constrained small cells with dense BS can be used to access all the UEs. Generally, to respond to the changing mobile market, 5G is expected to open new roles in the future mobile business ecosystem through the introduction of local 5G operators such as the recent micro operation.

3.2 5G eMBB Propagation Channel

5G eMBB network is expected to provide service in dense areas like, urban and sub-urban in which there are many users which mean there will be many BSs per cell. Since users are in urban and sub-areas, there will be buildings and factories which can interrupt and obstruct the signal transmission. So, practical channels contain a mix of deterministic LoS component and a random NLoS component. Since the SE of the channel between a particular UE and its serving BS, can potentially serve multiple UEs, say K UEs, simultaneously in each cell and achieve a sum SE that is the SE of all *UE SE* expressions.

Since the intra-cell interference is stronger than the inter-cell interference this must be suppressed if an increase in SE is actually to be achieved and provided. Space-division multiple access (SDMA) is conceived to handle the co-user interference in a cell by using multiple antennas at the BS to reject interference by spatial processing. We will now analyze a cellular network with SDMA transmission by assuming that there are K active UEs in each cell. Notice that the subscript indicates the identity of the UE, while the superscript is the index of the receiving BS. The DL channel response between the BS in cell l and its k^{th} desired UE is denoted by [16]

$$\left(h_{lk}^{l}\right)^{H}, \text{ for } k = 1, \ldots K. \tag{3.1}$$

The transpose represents the fact that we are now looking at the channel from the opposite direction, while the complex conjugate is added for notational convenience.

3.4.1 LoS Propagation channel Model

LoS propagation is a propagation environment in which the channel responses are deterministic as shown in Figure (3.1); the propagation when the transmitter single antenna UE and receiver BS with M-antennas are in direct line of sight.

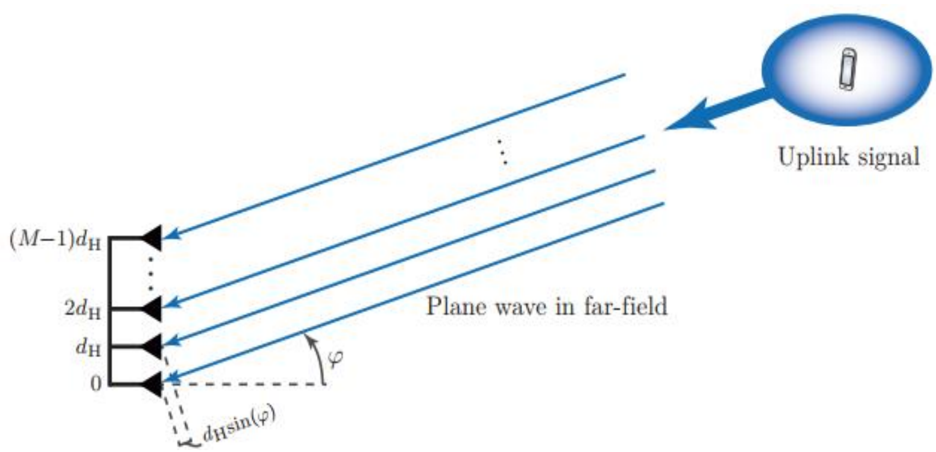

Figure 3.1: LoS Propagation environment [17]

The LoS channel response between UE k in cell j and the BS in cell l is modeled as;

$$h_{jk}^{l} = \sqrt{\beta_{j}^{l}} \left[1 \; e^{2\pi j d_H \sin(\varphi_{jk}^{l})} \ldots e^{2\pi j d_H (\mathrm{M}-1)\sin(\varphi_{jk}^{l})} \right]^{T} \tag{3.2}$$

Where, $\varphi_{jk}^{l} \in [0, \pi)$ is the azimuth angle relative to the boresight of the transmitting BS. The processing vector supports to maximize the SEs in massive MIMO systems. Since there are many users in many cells, the sum SE is the summation over the *K* UEs' SEs. The LoS SE expression, can be derived from the Wyner model which is initially proposed by Aaron Wyner and studied for analyzing fading channels [35]. To start with the lower bound SE in the UL of LoS propagation environment, we notice that $\left\|h_{lk}^{l}\right\|^{2} = \beta_{lk}^{l} M$ since each element of the channel response has squared magnitude, β_{lk}^{l} . We start by focusing on all UEs SE in multi-cells environment, as in (3.3);

$$\mathrm{SE} = \log\left(1 + \frac{p\left\|h_{jk}^{l}\right\|^{2}}{\sum_{l=1}^{L}\sum_{\substack{i=1 \\ i\neq k}}^{K} p \frac{\left|\left(h_{jk}^{l}\right)^{H} h_{li}^{l}\right|^{2}}{\left\|h_{jk}^{l}\right\|^{2}} + \sum_{l=1}^{L}\sum_{i=1}^{K} p \frac{\left|\left(h_{jk}^{l}\right)^{H} h_{li}^{l}\right|}{\left\|h_{jk}^{l}\right\|^{2}} + \sigma^{2}} \right) \tag{3.3}$$

The SE expressions in the deterministic LoS case can be obtained by summing up (3.3) in all the UEs SE over all multi-cells, and this becomes

$$SE_{l}^{LoS} = \sum_{l=1}^{L}\sum_{k=1}^{K} \log_{2}\left(1 + \frac{p\left|\left(h_{lk}^{l}\right)^{H} \frac{h_{lk}^{l}}{\left\|h_{lk}^{l}\right\|}\right|^{2}}{\sum_{l=1}^{L}\sum_{\substack{i=1 \\ i\neq k}}^{K} p\left|\left(h_{lk}^{l}\right)^{H} \frac{h_{li}^{l}}{\left\|h_{li}^{l}\right\|^{2}}\right| + \sum_{l=1}^{L}\sum_{i=1}^{K} p\left|\left(h_{lk}^{l}\right)^{H} \frac{h_{li}^{l}}{\left\|h_{li}^{l}\right\|^{2}}\right| + \sigma^{2}} \right) \tag{3.4}$$

With $h = \left\|h_{jk}^{l}\right\|$ and υ being the sum of all interferences. Where, f is the frequency reuse factor and s is the coherence block length. Next by utilizing the facts that

$$\left\|h_{lk}^{l}\right\|^{2} = \beta_{lk}^{l} M \tag{3.5}$$

$$\frac{\left|\left(h_{lk}^{l}\right)^{H} h_{jk}^{j}\right|^{2}}{\left\|h_{jk}^{j}\right\|^{2}} = \beta_{l}^{j} g\left(\varphi_{ji}^{j}, \varphi_{lk}^{j}\right) \; for \; 0,1,\ldots,L \tag{3.6}$$

The SE in ($\left[b/s/Hz/cell\right]$) is found to be

$$SE_{l}^{LoS} = \sum_{l=1}^{L}\sum_{k=1}^{K}\log_{2}\left(1+\frac{M}{\sum_{l=1}^{L}\sum_{\substack{i=1\\ i\neq k}}^{K} g\left(\varphi_{lk}^{l},\varphi_{li}^{l}\right)+\bar{\beta}\sum_{l=1}^{L}\sum_{i=1}^{K} g\left(\varphi_{lk}^{l},\varphi_{l'k}^{l}\right)+\frac{1}{SNR_{l}}}\right) \tag{3.7}$$

In the LoS case, SDMA results in the summation of *K* SE expressions, one per desired UE. The desired signal gains inside the logarithms increase linearly with *M* and thus every UE experiences the full array gain when using MR processing. Each interference term has the same form, thus one can expect the interference to be the lowest when the UEs have well-separated angles. The function $g\left(\varphi,\psi\right)$ decreases as $1/M$ for any $\sin(\varphi)\neq\sin(\psi)$. In conjunction with the array gain of the desired signal, we can thus serve multiple UEs and still maintain roughly the same SINR per UE if *M* is increased proportionally to $\sqrt{K}$ counteract the increased interference [13].

If the BS uses MR processing the UEs in cell l know their respective effective channels

$$\left(h_{lk}^{l}\right)^{H} w_{lk}\,, \tag{3.8}$$

And the interference variance, then an achievable DL SE in the LoS case is

$$SE = \sum_{\substack{l=1\\ l\neq l'}}^{L}\sum_{\substack{k=1\\ k\neq i}}^{K}\log_{2}\left(1+\frac{p\left|\left(h_{lk}^{l}\right)^{H}\frac{h_{li}^{l}}{\left\|h_{li}^{l}\right\|}\right|^{2}}{\sum_{\substack{l=1\\ l'\neq 1}}^{L}\sum_{\substack{i=1\\ i\neq k}}^{K} p\left|\left(h_{lk}^{l}\right)^{H}\frac{h_{li}^{l}}{\left\|h_{li}^{l}\right\|}\right|^{2}+\sum_{l'=1}^{L}\sum_{i=1}^{K} p\left|\left(h_{li}^{l'}\right)^{H}\frac{h_{l'i}^{l'}}{\left\|h_{l'i}^{l'}\right\|}\right|^{2}+\sigma^{2}}\right) \tag{3.9}$$

With $h=\left\|h_{lk}^{l}\right\|$ and v being the sum of all interference terms. By utilizing the facts that

$$\left\|h_{lk}^{l}\right\|^{2} = \beta_{lk}^{l} M \;\;, \tag{3.10}$$

$$\frac{\left|\left(h_{lk}^{j}\right)^{H} h_{ji}^{j}\right|^{2}}{\left\|h_{ji}^{j}\right\|^{2}} = \beta_{lk}^{j}\left(\varphi_{ji}^{j}, \varphi_{lk}^{j}\right) \tag{3.11}$$

For j= 1 . . . L, the SE in the LoS is found as;

$$SE^{LoS} = \sum_{\substack{l=1 \\ l' \neq l}}^{L} \sum_{\substack{k=1 \\ i \neq i}}^{K} \log_2 \left(1 + \frac{M}{\sum_{\substack{l=1 \\ l' \neq l}}^{L} \sum_{\substack{i=1 \\ i \neq k}}^{K} g\left(\varphi_{li}^{l}, \varphi_{lk}^{l}\right) + \bar{\beta} \sum_{l'=1}^{L} \sum_{i=1}^{K} g\left(\varphi_{l'i}^{l'}, \varphi_{lk}^{l'}\right) + \frac{1}{SNR}} \right) \quad (3.12$$

3.4.2 NLoS Propagation Channel Model

In the NLoS case propagation environments, the channel responses are random variables that change over time and frequency. The corresponding channel response between UE k in cell j and the BS l is modeled as

$$h_{jk}^{l} \sim N\left(0_M, \beta_j^l I_M\right) \tag{3.13}$$

And assumed to be statistically independent between UEs. The Wyner model is assumed in which, the transmitter and UE are located each other at a distant points, and the average channel gain is assumed to be the same for all UEs in cell j [35]. When the number of paths is large, a phenomenon is known as small-scale fading is found and is a microscopic effect caused by small variations in the propagation environment. The variance β_{jlk}^{l} is interpreted as the macroscopic large scale fading, which includes shadowing, antenna gains and penetration losses in NLoS propagation environment. The channel responses from the desired and interfering UEs can then be represented by the vectors $h_l^l \in \mathbb{C}^M$ and $h_j^l \in \mathbb{C}^M$ respectively. The m^{th} element of each vector is the channel response observed at the BS antenna, for m=1. . . M.

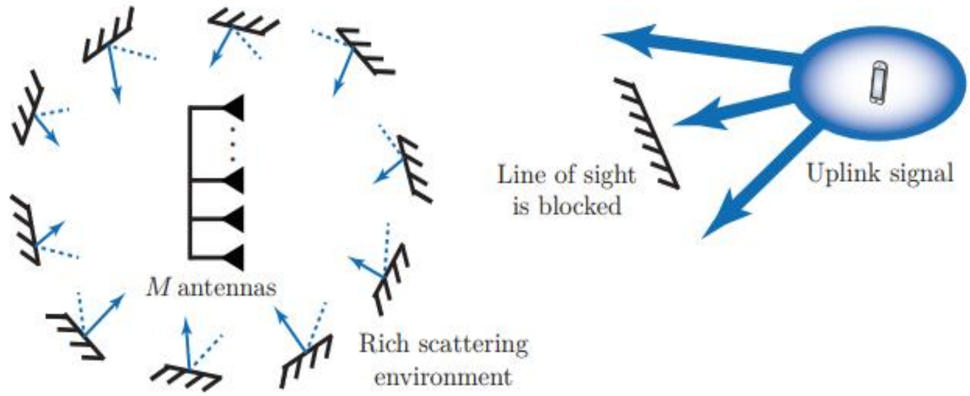

Figure 3.2: NLoS Propagation, the signal finds multiple paths via scattering objects.

The BS is surrounded by many scattering objects so that the UE location has no impact on the spatial directivity of the received signal. The benefits of having multiple antennas at the BS appear when the BS knows the channel response of the desired UE.

This knowledge enables the BS to coherently combine the received signals from all antennas. Estimation of the channel response is thus a key aspect in multi antenna systems. With NLoS channels, an achievable DL sum SE [bit/s/Hz/cell] and a closed-form lower bound can be derived. Since the NLoS channels are random and in this case an achievable SE (with $H = \left\| h_{lk}^{l} \right\|$ and Z containing,

$$\frac{\left| \left(h_{lk}^{j} \right)^{H} h_{ji}^{j} \right|^{2}}{\left\| h_{ji}^{j} \right\|^{2}} \quad \text{For all} \left(j, \mathrm{i} \right): \tag{3.14}$$

And provides the achievable SE which is given

$$SE_{l}^{NLoS} = \sum_{l=1}^{L} \sum_{k=1}^{K} \mathrm{E} \left\{ \log_{2} \left(1 + \frac{p \left\| h_{lk}^{l} \right\|^{2}}{\sum_{l=1}^{L} \sum_{\substack{i=1 \\ i \neq k}}^{K} p \frac{\left| \left(h_{lk}^{l} \right)^{T} h_{li}^{l} \right|^{2}}{\left\| h_{lk}^{k} \right\|^{2}} + \sum_{l=1}^{L} \sum_{i=1}^{K} p \frac{\left| \left(h_{lk}^{l} \right)^{T} h_{l'i}^{l} \right|^{2} + \sigma^{2}}{\left\| h_{lk}^{l} \right\|^{2}}} \right) \right\} \tag{3.15}$$

For UE k by dividing each term in the SINR by $\left\| h_{lk}^{l} \right\|^2$. Next we compute the expectation of the inverse of the SINR in (3.15). Which becomes

$$E\left\{ \frac{\sum_{\substack{l=1 \\ l'\neq 1}}^{L} \sum_{\substack{k=1 \\ i\neq k}}^{K} p \frac{\left| \left(h_{lk}^{l} \right)^{H} h_{li}^{l} \right|^2}{\left\| h_{lk}^{l} \right\|^2} + \sum_{\substack{l=1 \\ l'=1}}^{L} \sum_{\substack{k=1 \\ i=1}}^{K} p \frac{\left| \left(h_{lk}^{l} \right)^{H} h_{l'i}^{l} \right|^2}{\left\| h_{lk}^{l} \right\|^2}}{p \left\| h_{lk}^{l} \right\|^2} \right\} \tag{3.16}$$

$$= \frac{p(\mathrm{K}-1)\beta_{lk}^{l} + pK\beta_{l'k}^{l} + \sigma^2}{p(\mathrm{M}-1)\beta_{lk}^{l}} \tag{3.17}$$

$$= \frac{(\mathrm{K}-1) + \mathrm{K}\,\bar{\beta} + \frac{1}{SNR}}{M-1} \tag{3.18}$$

Now, by utilizing the facts that

$$\frac{\left| \left(h_{lk}^{l} \right)^{H} h_{jk}^{l} \right|^2}{\left\| h_{lk}^{l} \right\|^2} \tag{3.19}$$

Is independent of h_{lk}^{l}, and has mean value β_{jk}^{l}, whenever, $(\mathrm{j},\mathrm{i}) \neq 0,$ and

$$E\left\{ \frac{1}{\left\| h_{lk}^{l} \right\|^2} \right\} = \frac{1}{(\mathrm{M}-1)\beta_{lk}^{l}} \tag{3.20}$$

The expectation in (3.20) can be found from the standard results of the inverse of a^2 distribution. We can now apply Jensen's equality and utilize (3.19) and (3.20) to compute the lower bound SE as;

$$SE_l^{NLoS} = \sum_{l=1}^{K}\sum_{k=1}^{K} \mathrm{E}\left\{ \log_2\left(1+ \frac{p\left\|h_{lk}^l\right\|^2}{\sum_{l=1}^{L}\sum_{\substack{i=1\\ i\neq k}}^{K} p\frac{\left|\left(h_{lk}^l\right)^H h_{li}^l\right|^2}{\left\|h_{lk}^l\right\|^2} + \sum_{\substack{l=1\\ l'=1}}^{L}\sum_{\substack{k=1\\ i=1}}^{K} p\frac{\left|\left(h_{lk}^l\right)^H h_{l'i}^l\right|^2}{\left\|h_{lk}^l\right\|^2} + \sigma^2} \right)\right\} \tag{3.21}$$

By utilizing the convexity of $\log_2(1+1/a)$ with respect to a, which is the inverse SNR in this case,

$$SE^{NLoS} \geq K\log_2\left(1+\left(\frac{(K-1)+K\bar{\beta}+\frac{1}{SNR}}{M-1}\right)^{-1}\right) \tag{3.22}$$

Using (3.19) and assuming that the SE bound is the same for all the UEs, the Lower bound SE expression is finally, found to be;

$$SE^{NLoS} \geq K\log_2\left(1+\frac{M-1}{(\mathrm{K}-1)+\mathrm{K}\bar{\beta}+\frac{1}{SNR}}\right) \tag{3.23}$$

Due to the appearance of greater amounts of intra-cell and inter-cell interferences. The drawback of SDMA is seen from the denominator, where the interference terms contain contributions from *K-1* intra-cell UEs and *K* inter-cell UEs. Since the transmit precoding reduces the MISO channels to the effective channel gain. With $H = \left\| h_{lk}^{l} \right\|$ And Z containing $\frac{\left| \left(h_{lk}^{j} \right)^{H} h_{ji}^{j} \right|^{2}}{\left\| h_{ji}^{j} \right\|^{2}}$ for all j, i.

$$SE^{NLoS} = \sum_{l=1}^{L} \sum_{k=1}^{K} E\left\{ \log_2 \left(1 + \frac{p \left| \left(h_{lk}^{l} \right)^{H} \frac{h_{lk}^{l}}{\left\| h_{lk}^{l} \right\|} \right|^{2}}{\sum_{\substack{l=1 \\ l \neq l'}}^{L} \sum_{\substack{i=1 \\ i \neq k}}^{K} p \left| \left(h_{lk}^{l} \right)^{H} \frac{h_{li}^{l}}{\left\| h_{li}^{l} \right\|} \right|^{2} + \sum_{l'=1}^{L} \sum_{i=1}^{K} p \left| \left(h_{lk}^{j} \right)^{H} \frac{h_{li}^{j}}{\left\| h_{li}^{j} \right\|} \right|^{2}} \right) \right\} \tag{3.24}$$

Now let's begin computing the expectation of the inverse of the SNR in (3.24), which is

$$E\left\{ \frac{\sum_{\substack{l=1 \\ l' \neq l}}^{L} \sum_{\substack{i=1 \\ i \neq k}}^{K} p \left| \left(h_{lk}^{l} \right)^{H} \frac{h_{li}^{l}}{\left\| h_{li}^{l} \right\|} \right|^{2} + \sum_{l'=1}^{L} \sum_{i=1}^{K} p \left| \left(h_{lk}^{j} \right)^{H} \frac{h_{ji}^{j}}{\left\| h_{ji}^{j} \right\|} \right|^{2} + \sigma^{2}}{p \left\| h_{lk}^{l} \right\|^{2}} \right\} \tag{3.25}$$

$$= \sum_{\substack{l=1 \\ l' \neq l}}^{L} \sum_{\substack{i=1 \\ k \neq i}}^{K} E\left\{ \left| \frac{\left(h_{lk}^{l} \right)^{H}}{\left\| h_{lk}^{l} \right\|} \frac{\left(h_{li}^{l} \right)}{\left\| h_{li}^{l} \right\|} \right|^{2} \right\} + \left(\sum_{l=1}^{L} \sum_{i=1}^{K} E\left\{ \left| \frac{\left(h_{li}^{j} \right)^{H} h_{ji}^{j}}{\left\| h_{ji}^{j} \right\|} \right|^{2} \right\} + \frac{\sigma^{2}}{p} \right) E\left\{ \frac{1}{\left\| h_{lk}^{l} \right\|^{2}} \right\} \tag{3.26}$$

$$= \frac{K-1}{M} + \frac{K \beta_{lk}^{j} + \frac{\sigma^{2}}{p}}{(M-1) \beta_{lk}^{l}} \tag{3.27}$$

Where the first expectation is computed by utilizing the fact that $\left| \left(h_{lk}^{l} \right)^{H} h_{li}^{l} \right|^{2} \Big/ \left(\left\| h_{lk}^{l} \right\|^{2} \left\| h_{li}^{l} \right\|^{2} \right)$ is beta-distributed with parameters 1 and *M*, which implies that the expectation is 1/*M*. The second expectation follows from the fact that $\left(h_{lk}^{j} \right)^{H} h_{li}^{l} \Big/ \left\| h_{li}^{l} \right\| \sim N_{\mathbb{C}} \left(0, \beta_{lk}^{j} \right)$.

By applying Jensen's in equality we obtain that expression for SE in the DL is lower bounded as

$$\sum_{l=1}^{L}\sum_{k=1}^{K}\log_2\left(1+\left(\frac{K-1}{M}+\frac{K\beta_{lk}^{j}+\frac{\sigma^2}{p}}{(M-1)\beta_{lk}^{l}}\right)^{-1}\right) \tag{3.28}$$

$$SE^{NLoS} \geq K\log_2\left(1+\frac{(M-1)}{(K-1)\frac{M-1}{M}+K\bar{\beta}+\frac{1}{SNR}}\right) \tag{3.29}$$

The NLoS case only differs in the extra multiplicative term M-1/M in the denominator of (3.29), which is almost one for large M. The LoS case only differs in the angles that appear in each expression. We have assumed that the inter-cell interference is equally strong and the same in the UL and DL across the entire cells. In general, there are also differences in the average channel gains. The array gain is M with MR processing in both UL and DL.

3.5 Network Model and Spectral Efficiency

The majority of research works in the literature discussed so far in section (1.2), assumed the standard path loss model where received power decays like $d^{-\alpha}$ over a distance d, where α is called the path loss component. This standard path loss model is idealized and in most scenarios α is itself a function of distance typically an increasing one. In practical, different regimes could be observed; distance independent near field $\alpha = 0$, free space regime, $\alpha_1 = 2$ finally attenuated regime $\alpha_2 > 2$. Propagation environments and fading distribution play in identifying network operating regimes for which an increase, saturation, or decrease of the through put is observed as the network is densified.

We consider the UL of a cellular network where in the BSs are spatially distributed at locations $\{z_i\} \in \mathbb{R}^2$ within a compact geometric area according to $\Phi_D = \{z_i; i \in N\} \subset \mathbb{R}^2$ of intensity $D\left[BS/\mathrm{k}m^2\right]$. As shown in figure (3.3) a typical network model; let A be the network area of interest, and the average number of deployed BSs is simply given by $\mathrm{E}_{\{z_i\}}\{\Phi_D\} = DA$. It is assumed that each UE is connected to the closest BS in a cell.

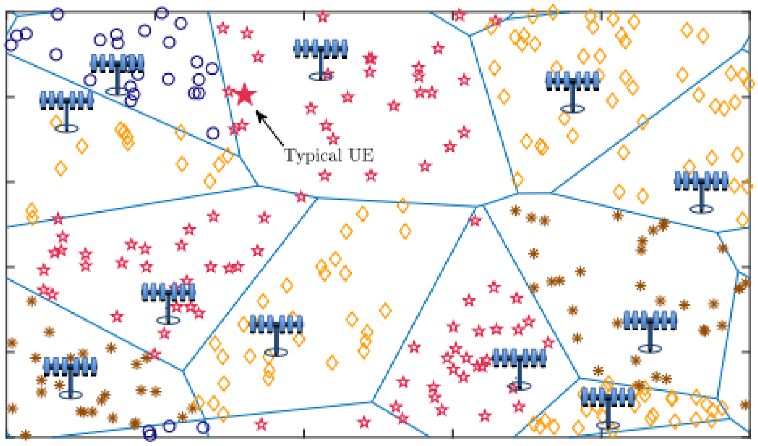

Figure 3.3: Cellular network model, where BSs serve K randomly located UEs

The UEs of different cells sharing the same pilot subset Φ_l are depicted with the same marker and color. Without loss of generality, we assume that the typical UE, which is statistically representative for any other UE in the network, has an arbitrary index *k* and is connected to an arbitrary BS *j*. The network operates according to a synchronous time-division-duplex protocol. We denote by *B*C [Hz] and *T*c [s] the coherence bandwidth and time, respectively. Then, the coherence block is composed of $\tau_c = B_c T_c$. In each coherence block, τ_p samples are used for acquiring channel state information by means of UL pilot sequences, whereas τ_u and τ_d samples are used for payload transmission in the UL and downlink (DL), respectively. We assume that $\tau_c = fK$ with $f \geq 1$ being the pilot reuse factor [26].

3.5.1 Area Spectral Efficiency

Since the typical UE is the representative for any other UE in the network, the area spectral efficiency ASE is obtained as

$$ASE = DK\ (SE)\ in[\text{bits/ se/ Hz/ km}^2]$$

Where SE denotes the average UL spectral efficiency of the typical UE k in cell j and is obtained averaging over different UE positions, pilot allocations and channel realizations. The multiplicative factor K accounts for the sum SE of all UEs in cell j and D the BS density in km^2. A lower bound on SE which hold for any processing scheme, UE positions and pilot allocations is modelled as follows;

$$SE \geq \zeta\left(1-\frac{Kf}{\tau_c}\right)\mathrm{E}_{\{d,h,a\}}\left\{\log_2\left(1+SINR\right)\right\} \tag{3.30}$$

Where $SINR$ is the instantaneous $SINR$ given by

$$SINR = \frac{p_{jk}\left|w_{jk}^H \hat{h}_{jk}^j\right|^2}{w_{jk}^H\left(\sum_{l\in\Phi_D}\sum_{\substack{i=1\\(l,i)\neq(j,k)}}^{K} p_{li}\hat{h}_{li}^{jH} + \sum_{l\in\Phi_D}\sum_{i=1}^{K} p_{li}\left(\beta_{li}^j-\gamma_{li}^j\right)I_M + \sigma^2 I_M\right)w_{jk}} \tag{3.31}$$

Since distance dependent path loss model is used as explained in (2.12) β_{li}^j can be substituted by $\gamma_n = \left(d_{li}^j\right)^{-\alpha_n}$. Thus the expression in (3.31) becomes

$$SINR = \frac{p_{jk}\left|w_{jk}^H \hat{h}_{jk}^j\right|^2}{w_{jk}^H\left(\sum_{l\in\Phi_D}\sum_{\substack{i=1\\(l,i)\neq(j,k)}}^{K} p_{li}\hat{h}_{li}^{jH} + \sum_{l\in\Phi_D}\sum_{i=1}^{K} p_{li}\left(\gamma_n\left(d_{li}^j\right)^{-\alpha_n}-\gamma_{li}^j\right)I_M + \sigma^2 I_M\right)w_{jk}} \tag{3.32}$$

The expectation $\mathrm{E}_{\{d,\mathrm{h},\mathrm{a}\}}\{.\}$ is computed with respect to UE positions, channel realizations and pilot allocations. The pre-log factor accounts for pilot overhead. The optimal vector w_{jk} that maximizes (3.30) is given by the instantaneous UL SINR in (3.32) for a typical UE k in cell j is maximized by

$$w_{jk}^{M-MMSE} = \left(\sum_{l\in\Phi_D}\sum_{i=1}^{K} p_{li}\left(\hat{h}_{li}^j\left(\hat{h}_{li}^j\right)^H + \left(\gamma_n\left(d_{li}^j\right)^n-\gamma_{li}^j\right)I_M\right)+\sigma^2 I_M\right)^{-1} p_{jk}\hat{h}_{li}^j \tag{3.33}$$

The vector of the MR processing is given by $w_j^{MR} = \hat{H}_j^j$ is obtained for low SINR Whereas the vector for ZF processing is

$$w_{li}^{zf} = \hat{H}_j^j\left(\left(\hat{H}_j^j\right)^H H_j^j\right)^{-1} \tag{3.34}$$

Since the UL channel is estimated using MMSE as discussed in section (2.6) the UL powers can be chosen as $p_{jk} = \frac{p_0}{\beta_{jk}^{j}}$ and ZF processing is used since it provides balance in performance and computational complexity. So the lower bound expression of the UL average ergodic channel capacity of the typical UE k in cell j computed as

$$SE = \zeta\left(1 - \frac{K\zeta}{\tau_c}\right)\log_2\left(1 + SINR\right) \tag{3.35}$$

Where

$$SINR = \frac{M - K}{\beta_{jk}^{j} + \left(M - K\right)\mu/\zeta} \tag{3.36}$$

β_{jk}^{j} Is the interference and is given by

$$\beta_{jk}^{j} = \left(K + \frac{1}{SNR}\right)\left(1 + \frac{\mu_1}{\zeta} + \frac{1}{SNR_p}\right) + \frac{K}{\zeta}\left(\mu_1^2 + \mu\right) + K\mu_1\left(1 + \frac{1}{SNR_p}\right) - K\left(1 + \frac{\mu}{\zeta}\right) \tag{3.37}$$

And μ_k *for* $k = 1, 2$

$$\mu_k = 2\sum_{n=1}^{N} \frac{\Gamma\left(2; \pi D R_{n-1}^2\right) - \Gamma\left(2; \pi D R_n^2\right)}{} + \frac{2c_n\left(k\right)}{\left(\pi D\right)^{\frac{k\alpha_n}{2} - 1}}\left(\Gamma\left(1 + \frac{k\alpha_n}{2}; \pi D R_{n-1}^2\right) - \Gamma\left(1 + \frac{k\alpha_n}{2}; \pi D R_n^2\right)\right)$$

(3.38)

With

$$c_n\left(k\right) = -\frac{R_n^{2-k\alpha n}}{k\alpha_n - 2} + \sum_{i=n+1}^{N}\left(\frac{\Upsilon_i}{\Upsilon_n}\right)^k \frac{R_{i-1}^{2-k\alpha_i} - R_i^{2-k\alpha_i}}{k\alpha_i - 2} \tag{3.39}$$

Notice that the numerator of SINR in (36) scales with *M* - *K* since each BS sacrifices *K* degrees of freedom for interference suppression within the cell. The pilot contamination term scales also with *M* - *K* and accounts for the coherent interference due to UEs that use take in to account pilot sequence used in the typical UE. Many of the interference terms increase with *K* since having more UEs leads to both more intra-cell and inter-cell interference due to the imperfect CSI and lack of multi-cell processing [25, 26].

3.6 Optimal Power Control Schemes

Different papers has been done on multi-cell massive MIMO systems power allocation techniques. Multi cell massive MIMO is a system in which inter-cell interference has to be modelled if a suboptimal per cell optimization solution is to be founded. Effective and computationally tractable power control is one of the unique features of Massive MIMO. Among other things, power control handles near-far effects, and it enables uniformly good service to the cell. Massive MIMO power control occurs on a long time scale because effective SINRs depend only on large-scale fading coefficients. The channel hardening discussed in section (2.2) makes power control techniques unique in 5G Massive MIMO systems. There is no need to adapt the transmit powers to small-scale fading variations, but only to the large-scale fading characteristics. In practice, the transmit power of a BS is limited by regulations and hardware constraints, which we model by a maximum total transmit power $P_{mzx}^{DL} \geq 0$ per BS. The resulting utility maximization problem is

$$\begin{aligned} &\underset{\rho_{11}\geq 0,\dots,\rho_{LK_L}\geq 0}{Maximize} \quad \left(SE_{11}^{DL}, \dots, SE_{LK_L}^{DL} \right) \\ &Subject\ to \quad \sum_{k=1}^{K} \rho_{jk} \leq P_{\max}^{DL},\ l = 1,\dots,L \end{aligned} \tag{3.40}$$

Where the DL transmit powers $\rho_{11},\dots,\rho_{LK_L}$ are the $\sum_{l=1}^{L} K_l$ optimization variables. The actual power transmitted by the BS is $\sum_{k=1}^{K} \rho_{lk}$.

This problem formulation can be used with any precoding techniques and keep the precoding vector fixed while optimizing the transmit powers. This unique characteristic of Massive MIMO makes advanced power allocation schemes that are practically feasible.

3.6.1 Geometric Optimization

It is one of the optimization problem which is used to solve and develop power control schemes. To enable the structured analysis and algorithmic development, it is convenient to write an optimization problem on the standard form [24]

$$\underset{x}{Maximize} \quad f_0(x)$$
$$Subject\ to \quad f_n(x) \leq 0 \quad n = 1, \ldots, N \tag{3.41}$$

Where the N functions $f_n \ : \mathbb{R}^V \to \mathbb{R}$ are called the constraint functions. Any constrained optimization can be reformulated on the standard form [24, 29], but the dimension of x might change in the reformulation.

Let $f_o \ and \ f_1 - 1, \ldots, f_N - 1$ are posynomial functions. Note that a function $f_n : \mathbb{R}_+^V \to \mathbb{R}$ is posynomial if it can be as

$$f_n(x) = \sum_{b=1}^{B} c_b x_l^{e_{2,b}} x_2^{e_{2,b}} \ldots x_V^{eV,b} \tag{3.42}$$

For some integer B, constants $c_b > 0$, and exponents

$$e_{1,b}, \ldots, e_{V,b} \in \mathbb{R} \text{ For, } b = 1, \ldots, B, where\, x = [x_1 x_2 \ldots x_V]^T \tag{3.43}$$

is a vector with non-negative elements.

3.6.2 Max-Product SINR Power Control

The idea behind this power control scheme is to maximize the product of the effective SINRs. Let's consider

$$\begin{aligned} \sum_{j=1} \sum_{k=1}^{K} SE_{jk}^{DL} &= \sum_{j=1} \sum_{k=1}^{K} \frac{\tau_d}{\tau_c} \log_2\left(1 + SINR_{lk}^{DL}\right) \\ &\geq \sum_{j=1} \sum_{k=1}^{K} \frac{\tau_d}{\tau_c} \log_2\left(SINR_{jk}^{DL}\right) = \frac{\tau_d}{\tau_c} \log_2\left(\prod_{j=1}^{L} \prod_{k=1}^{K} SINR_{jk}^{DL}\right) \end{aligned} \tag{3.44}$$

Which shows that this utility seeks to maximize a lower bound on the sum SE. This has little effect on UEs that support high SINRs, but underestimates the SEs of the weakest UEs. Hence, a maximization of the product of the SINRs leads to higher SEs for the weakest UEs, as compared to maximizing the sum SE. The max-product SINR utility also guarantees that every UE gets a non-zero SE. The Max-Product SINR problem for a value of a_{lk} and b_{lijk} is expressed as

$$\begin{aligned} & \underset{\rho_{11}\geq 0,\ldots,\rho_{LK_L}\geq 0, c_{11}\geq 0, c_L K_L \geq 0}{Maximize} && \prod_{l=1}^{K}\prod_{k=1}^{K} c_{lk} \\ & Subject\ \ to && \sum_{l=1}\sum_{k=1}^{K}\frac{c_{lk}\rho_{li}b_{lijk}}{\rho_{jk}a_{jk}} + \frac{c_{jk}\sigma_{DL}^{2}}{\rho_{jk}a_{jk}} \leq 1 \quad , \\ & && l=1,\ldots,L,\ \ k=1,\ldots,K \\ & && \sum_{k=1}^{K}\rho_{lk} \leq P_{\max}^{DL},\ l=1,\ldots,L \end{aligned} \tag{3.45}$$

There is a variety of tradeoffs between these extremes, represented either by weighing the SEs of the UEs differently in or by using alternative functions; for example, the geometric mean or the harmonic mean of the SE advocates a heuristic approach for maximizing the minimum SE locally in each cell, while allowing for different SE levels in different cells. This is made possible by neglecting coherent interference and assuming that every BS and at least one UE per cell transmit with full power. To understand the motivation behind maximizing the product of the effective SINRs, let us consider the DL and notice that. The resulting utility maximization problem is

$$\begin{aligned} & \underset{\rho_{11}\geq 0,\ldots,\rho_{LK_L}\geq 0}{Maximize} && U\left(SE_{11}^{DL},\ldots,SE_{LK}^{DL}\right) \\ & Subject\ to && \sum_{k=1}^{K}\rho_{jk} \leq P_{\max}^{DL},\ j=1,\ldots,L \end{aligned} \tag{3.46}$$

Where the DL transmit powers $\rho_{11},\ldots,\rho_{LK}$ are the $\sum_{j=1} K_l$ optimization variables. $\sum_{k=1}^{K}\rho_{lk}$, is the power transmitted by BS. This problem formulation can be used along with any precoding scheme and we keep the precoding vectors fixed while optimizing the transmit powers. It is mainly the macroscopic mobility of UEs that determines the time interval over which the channel statistics are static.

3.6.3 Max-min Fairness Power Control

Max-min fairness is one of the well-known power control schemes that are suitable for a network that is serving users with identical data demand. Applying network-wide max-min fairness in the multi-cell Massive MIMO setup provides a uniform SE for all $K \times L$ users. The optimization problem is formulated as

$$\begin{aligned} &\underset{\{\eta_{lk}\}}{maximize} \quad \min_{l,k} \quad SINR_{lk} \\ &Sunject\ to \qquad 0 \leq \eta_{lk} \leq 1,\ for\ all\, l,k. \end{aligned} \tag{3.47}$$

Form this we are maximizing the minimum SINR of weakest user in the whole network. To solve this problem we can write it in epigraph optimization form

$$\begin{aligned} &\underset{\{\eta_{lk}\},t}{\max imize} \quad t \\ &subject\ to \quad 0 \leq \eta_{lk} \leq 1,\ for\ all\ l,k. \end{aligned} \tag{3.48}$$

Now, we are maximizing an auxiliary variable t that indicates the SINR requirement of all the users in the network. These new constraint are linear constraints for a fixed value of t. Hence, to solve this problem, we can fix t and solve the corresponding linear optimization problem which can be solved efficiently using the standard solver, geometric programming [24].

Chapter 4

Simulation Results and Discussions

4.1. Simulation Assumptions

We simulate the SE in Massive MIMO system and take all non-negligible interference into account. The simulations results are obtained by computing the lower bound expressions for different parameter combinations. The simulation is done for different cases such as;

Case 1. Average SE for different propagation environments and fixed SNR, different interference levels as a function of BS antennas, M.

Case 2. Per-cell SE as function of number of UEs, different interference strength and different channel models**.**

Case 3. Per-cell SE for different pilot reuse factors and different BS antennas as a function of number of users.

Case 4. Average SE in different path loss models as a function of BS density.

Case 5. CDF of different power control schemes for fixed SINR, number of BS, and different UEs.

Finally the simulation is used for the analysis of spectral efficiency and the impact of different system parameters according to the model developed channel models in chapter three. The simulation is done for the following assumptions:

- ✓ The same frequency is reused in every cell of the network
- ✓ There is no any co-operation between different BSs
- ✓ Perfect synchronization is assumed

Table 4.2: Used path loss exponents for different environments

Propagation environment Type	Path loss exponent
Urban Area	2.7-3.5
In building LoS	1.6-1.8
Obstructed in building	4-6

List of various parameters used for simulation are presented in the table. In 4G mobile technology, assures the high mobility with high level speed of data rates and high capacity IP based services and application are standardized. Parameters are related with advanced LTE standardized and 3GPP [29].

Table 4.3: Value of different simulation parameters.

Simulation parameters	Values
Hexagonal network	Symmetric
Number of BS antennas	M
Number of users per cell	K
Bandwidth	B=50 MHz
Reciever nise powers	-94dBm
DL power/fixed	20dBm
Samples per coherence block length	200
Pilot reuse factor	1,3,4
Length of uplink pilot sequences	$\tau_p = fK$
SINR (fixed)	5dB accoriding to LTE standard
Number of realizations	1000

4.2 Average SE for different channel vs number of BS Antenna

Figure (4.1), shows the average SE as a function of the number of BS antennas when the SNR of the desired UE is fixed as a fucntion of BS antennas. Different interference levels are considered for comparison. Antenna spacin of 0.5 is used and the results are averaged over different independent UE angles, all being uniformly distributed. As moving from M=1, to M=10 there is an improvement in the average SE due to array gain. The lower bound with NLoS for number of BS antennas greater that 10 is very tight.

The SE for both propagation environment is a monotically increasing function of M and grwos without limit for large value of M. we can also observe that the difference between LoS ans NLoS is negligible due to the fact that the channel fading has smaller impact on the mutual information in between the transmitted and recived singal.

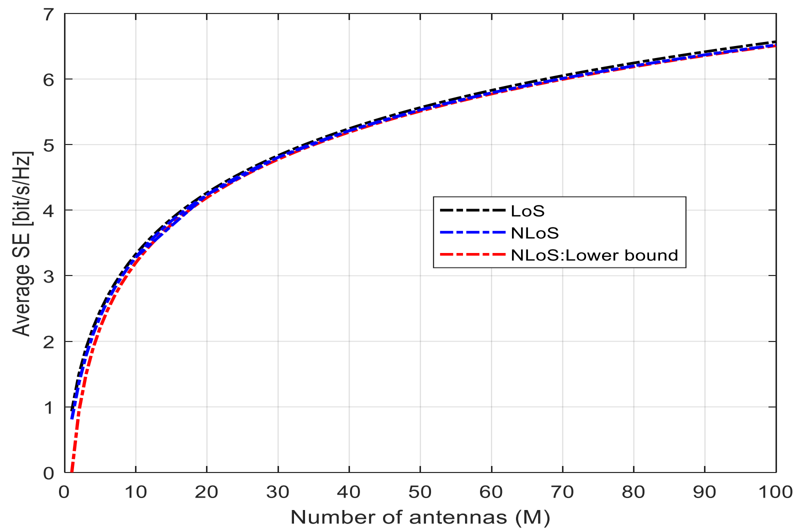

Figure (a): Average SE as a function of BS antenna for Interference level of -10dB.

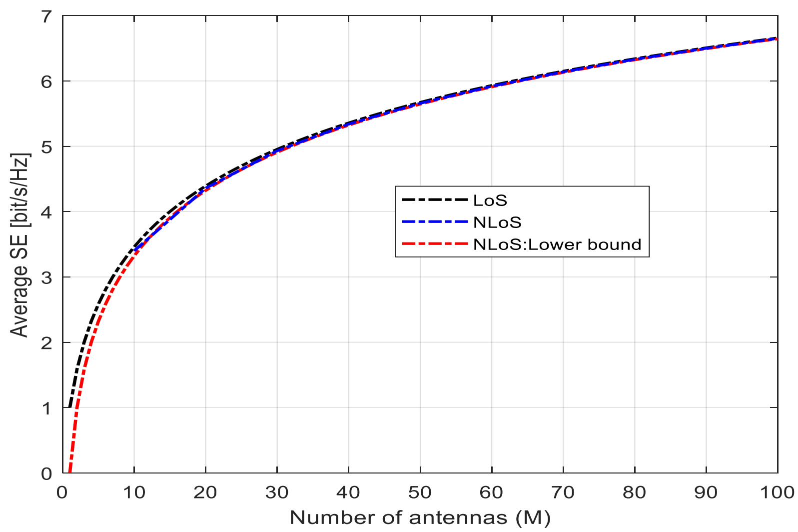

Figure (b) : Average SE as a function of BS antenna for Interference level of -20dB

Figure 4.1: Average SE as a function of number of BS antennas, M for different channel models

4.3 Per-cell SE for different Channel models as function of number of UEs

Figure (4.2) shows the SE of different propagation channels as a function of UEs. Comparing the two propagation environments, NLoS provides lower SE than LoS when using MR processing. But using ZF we get the opposite result.

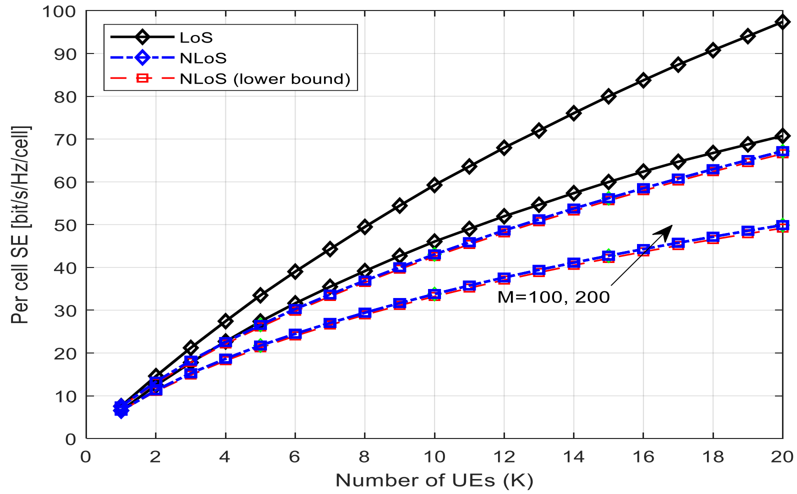

(a) MR processing

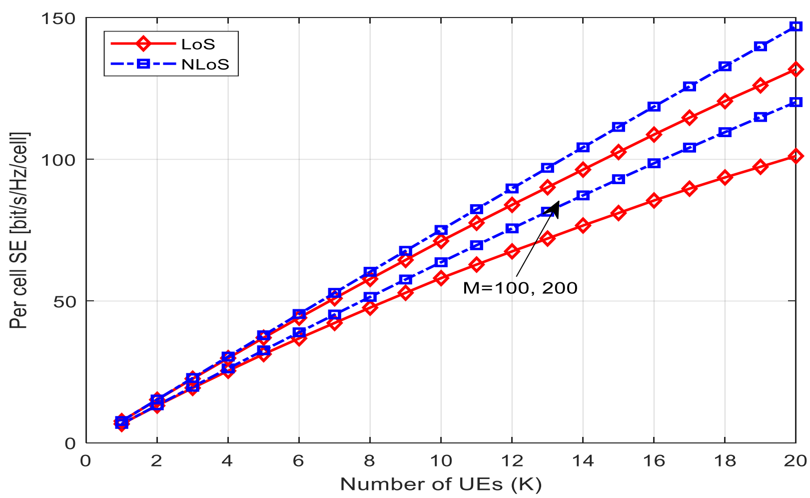

(b) ZF processing

Figure 4.2: Per cell SE for different channel models and different BS antennas as a function of number of UEs

4.4 Average SE for different Channel models as function of SNR Value

Figure (4.3) shows the average SE for different propagation envirnments as a function of SNR and under different interferecne level. The increase in SNR is the increase of the transmit power. We can have two different interference levels for compararing the chnnale models.

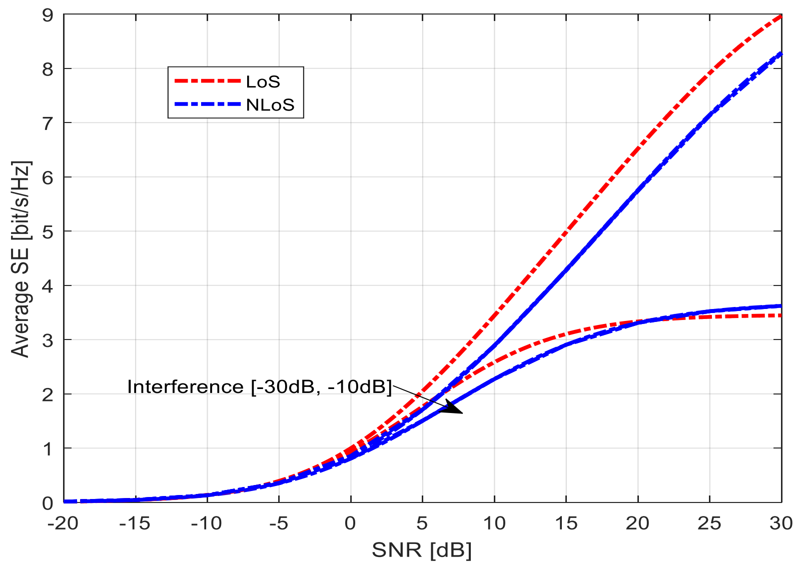

Figure 4.3: Impact of different interference levels for different channel models as a function of SNR Values

4.5 SE in different propagation channels with pilot reuse factor

Figure (4.4) shows the per cell SE for different pilot reuse factors, range of UEs and M=200. The average SE in a cell increases as the BS antenna increases for all the pilot reuse factors. Reusing pilots many times can lead to a loose in performance due to the interference of users singal form other cell which is called pilot contamination.

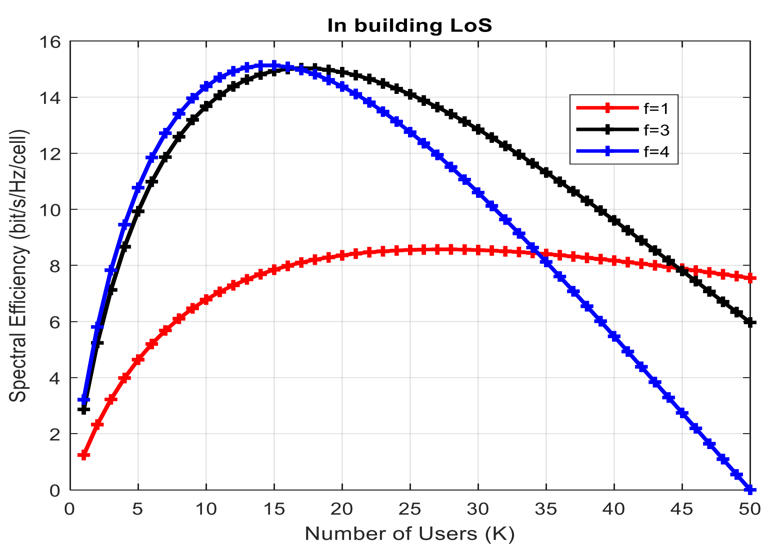

Figure 4.4: Per-cell SE for different pilot reuse factor in building LoS, M=200 using ZF

Figure (4.5) shows the average SE of different pilot reuse facotrs, varying number of users and BS antenna M=200 in obstructed building environments. The frequency reuse factor of f= 3 provides maximum per-cell SE when using ZF processing.

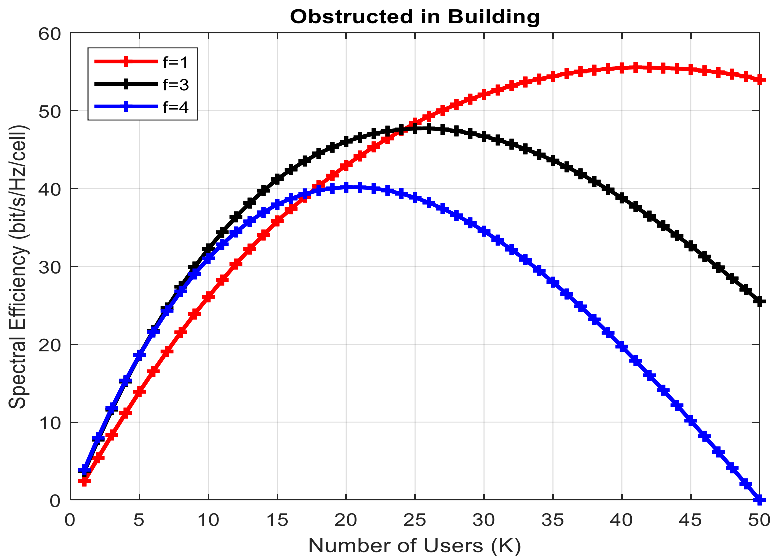

Figure 4.5: Per-cell SE in obstructed building for different reuse factors, BS antennas, M=100 using MR Processing

Figure (4.6) shows per-cell SE in urban areas with different pilot reuse factors. Pilot reuse factor of f=3, provides maximum SE using ZF processing for BS, M=100. But when we use maximum ration processing f=1 provides maximum performance and serves more UEs.

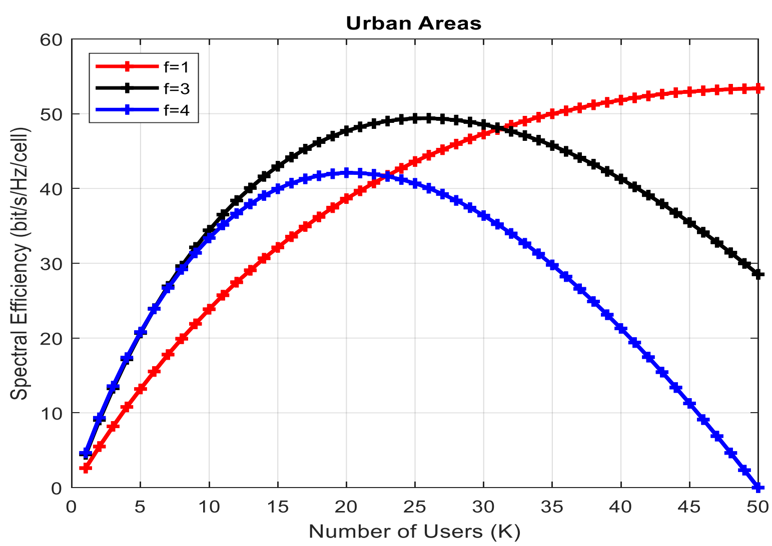

Figure 4.6: Per-cell SE in Urban area for different pilot reuse factors as a function of UEs

4.6 Spectral efficiency with different path loss models

Figure (4.7) shows the SE for different BS density and throughput of different processing techniques. It is observed that the SE is a non decreasing fucntion of base station desnity for all processing schemes in distance dependent path loss model. The figure in (b) is for distance independent path loss model as a function of BS density.

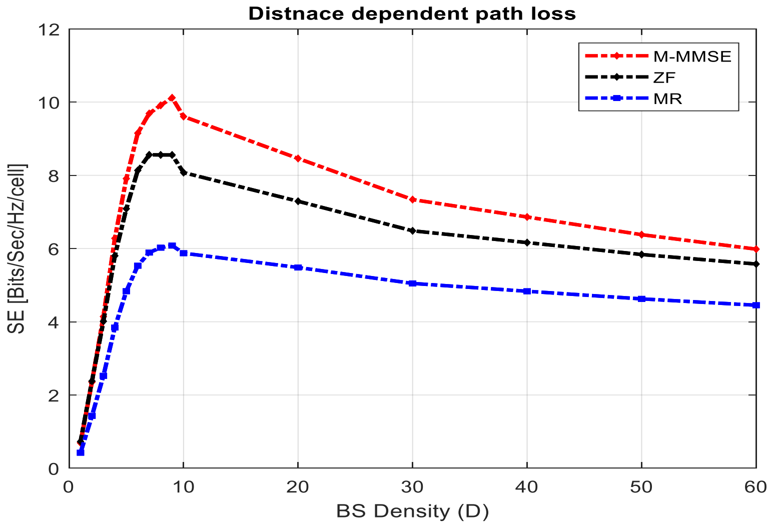

(a): SE in distance dependent path loss model

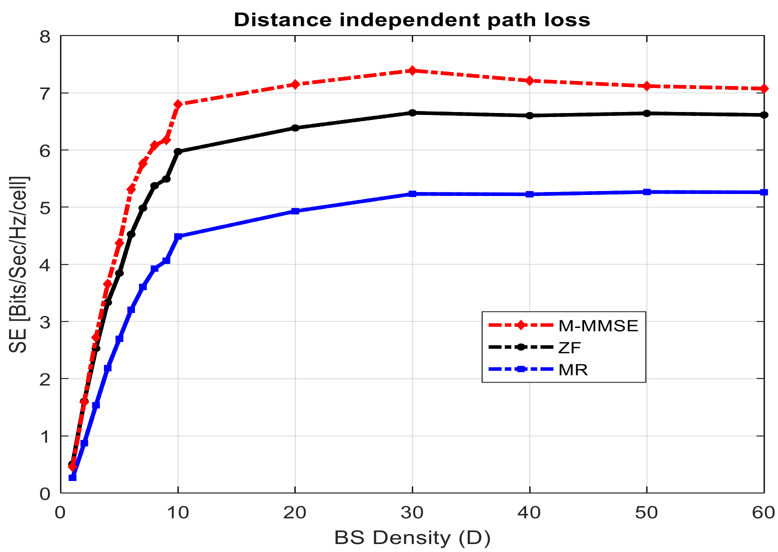

(b): SE in distance independent path loss model

Figure 4.7: SE as a function of BS density

Figure (4.8) shows SE for M-MMSE, ZF, and MR as a function of average area throughput for BS antenna, M=100 and UEs, K=10. We can see that the SE and throughput can increase at the same time. There is a variety of throughput and BS densities to maximize the SE.

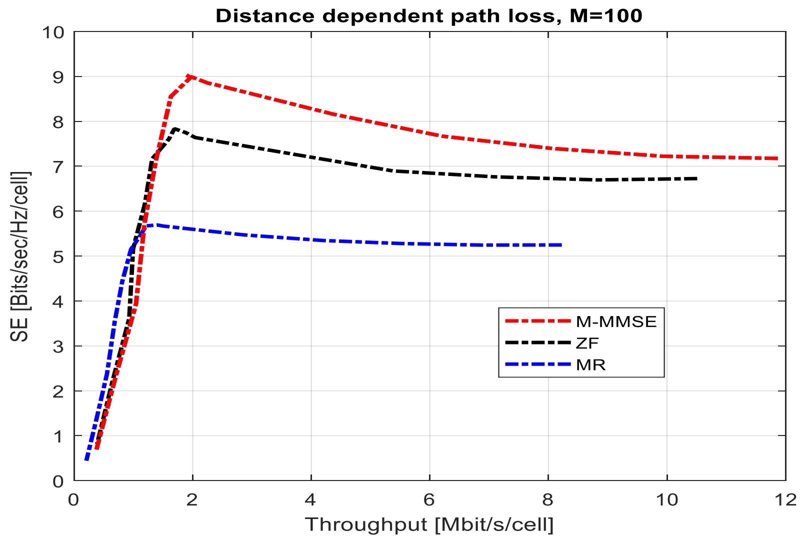

(a): SE in distance dependent path loss model

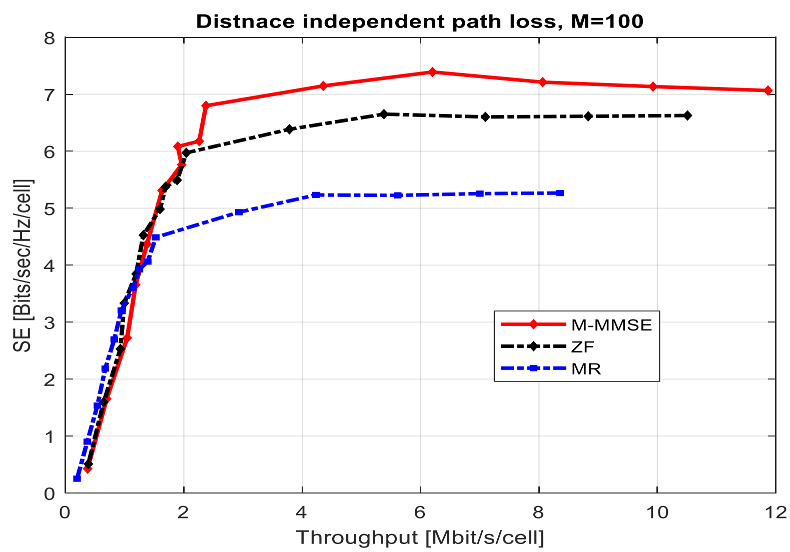

(b): SE in distance independent path loss model

Figure (4.8): SE as a function of throughput for different processing techniques

The figure shown in (4.9) is the closed form expression of the average SE provided in (3.36) for different processing techniques; (a) for distance dependet path loss model and (b) for distance independet path loss model. Although there is a gap between the lower and upper bounds, the curves behave exactly the same for any value of *D*.

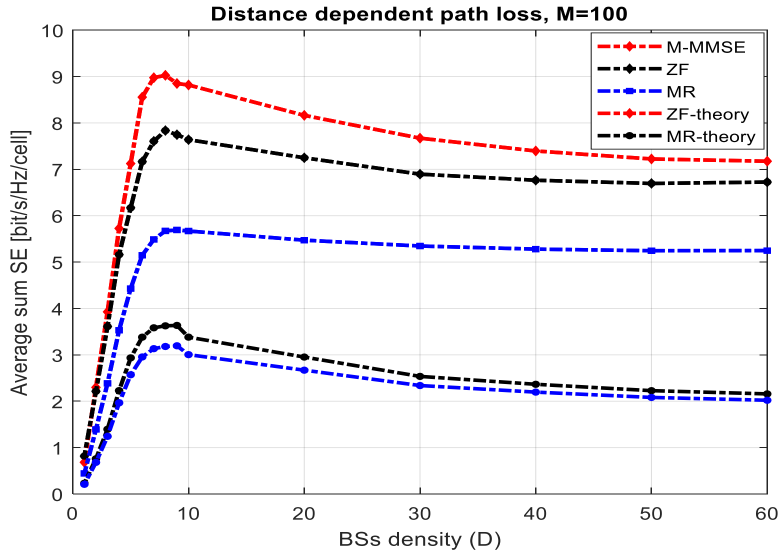

Figure (a): SE in distance dependent path loss model

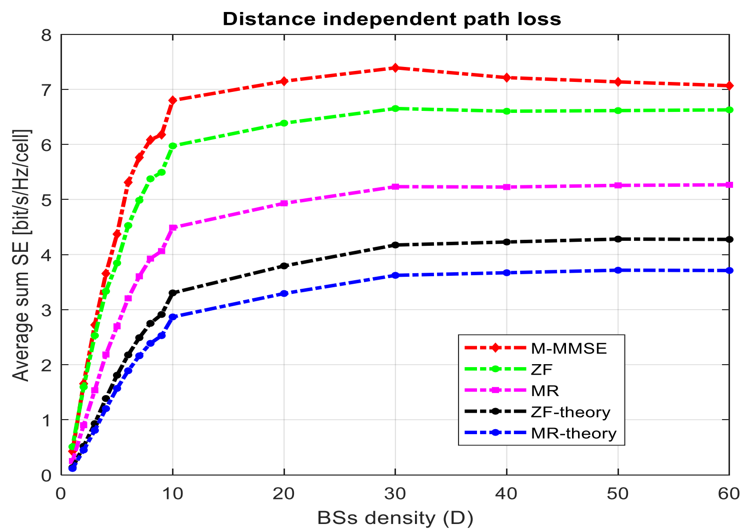

Figure (b): SE in distance independent path loss model

Figure 4.9: SE as a function of BS density for different Processing scheme

4.7 Per User SE with different power control techniques

Figure (4.9) shows the SE of each users, for different power control schemes. It is observed that the CDF of the max-product SINR is to the right of the fixed power control curve, which in turn is to right of the max-min fairness curve.

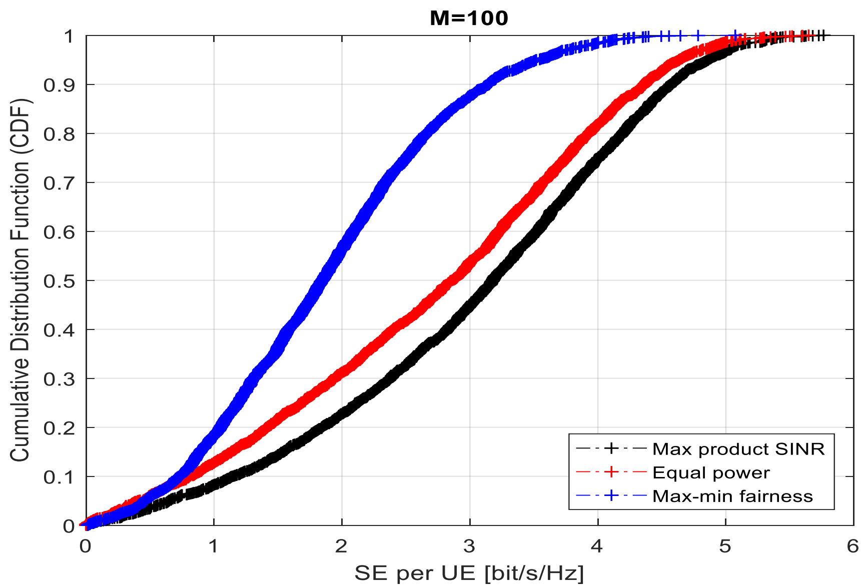

Figure 4.10: Per-user SE for different power control schemes for K=1o, M=100 using ZF

Figure (4.11) is with an increase of BS antennas M=200. The UEs spectral efficiency is increasing as the number of BS antennas increases for all power control schemes. CDF of all the Max-product SINR is to the right of the other power control schemes as before but with an increase of spectral efficiency. Max-min fairness provides better performance at SE close to zero. Still Max-product SINR is showing good UEs performance.

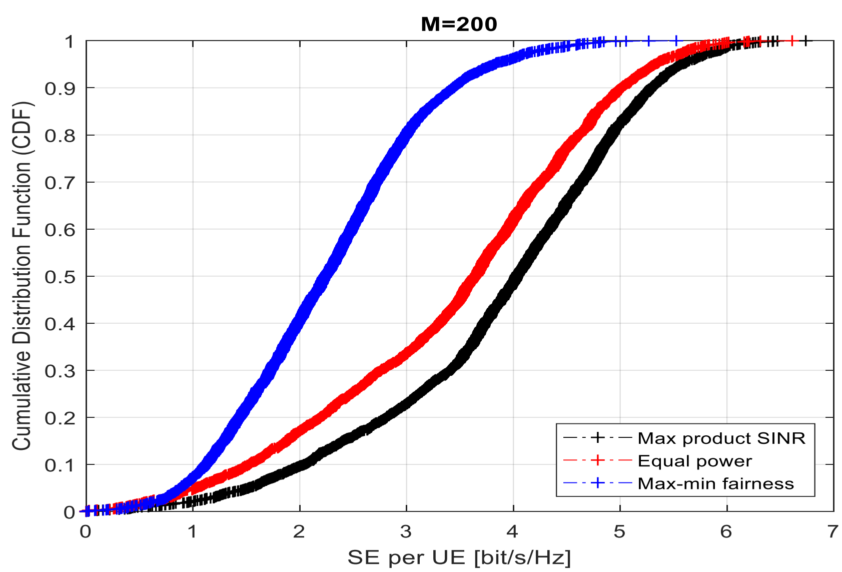

Figure 4.11: Per-user SE of different power control schemes for M=200 using ZF Processing

Chapter 5

Conclusion and Future work

5.1 Conclusion

Massive MIMO system introduces the opportunity of improving the spectral efficiency in 5G Mobile broadband networks. The system is able to use simple processing techniques like, ZF, MR, and M-MMSE both in the uplink and downlink. TDD protocol is used to simply channel make reciprocity.

In this thesis we have analyzed the spectral efficiency in 5G enhanced mobile broadband network under different propagation environments and also the UEs spectral efficiency with different power control schemes. Number of BS antenna is crucial to the performance. Conversely, number of terminals antenna degrade the performance due to user interference. As the number of terminals increases the mathematical complexity of SINR increases.

Generally, Massive MIMO in application to eMBB in LoS and NLoS is analyzed. Distance dependent path loss model is used in dense BS antennas. Both propagation channels provides the same performance as number of antennas grows. As number of BS antennas increases the array gain increases and the reusing of frequency factors also provides better performance because it is good in mitigating pilot contamination and interferences. Besides massive MU-MIMO can use a simple processing. We can also see that densification increases the SE in distance dependent path loss model. From the used processing schemes ZF provides balance between efficiency and complexity.

Finally, for the DL system power control schemes are analyzed to enhance the UEs spectral efficiency. It is found that the power control schemes greatly affect the SE distribution among the UEs. The max product SINR utility provides a good balance between sum SE and fairness. In this simulation, the max-product SINR power control provides better UEs performance.

5.2 Future Work

Here are list of recommendations to the possible extensions of the works of this thesis research:

- ✓ 5G enhanced mobile broadband service can be studied and deployed in the case of Ethiopia especially in urban and sub-urban areas.
- ✓ Massive MIMO system analyzed in this thesis considered non-cooperated BSs. Further works can be done with coordinated BS antennas which can improve the spectrum utilization efficiency.
- ✓ Additional advanced processing techniques can be implemented including low complexity channel estimation techniques. Also a practical channel model without interference such as the Nakagamim fading channel, the massive MIMO system with the linear precoding improves the performance with different parameters when the number of antennas increases.
- ✓ Linear and simple processing is assumed in this thesis, therefore it is desirable to study and corporate adaptive transmit beamforming which is a key to increase spectral and energy efficiency in very large antenna arrays
- ✓ An orthogonal transmission strategy has been considered in this work which can impact the spectrum utilization efficiency; it would be beneficial to deal it with non-orthogonal transmissions like, NOMA.
- ✓ Adaptive power algorithm can be investigated to improve and control the user’s power.

References

[1] M. Grant, CVX: Matlab software for disciplined, 2008.

[2] S. B. a. L. Vandenberghe, Convex Optimization, New york, NY, USA, 2004.

[3] Emil Bjornson, Jakob Hoydis, Luca Snaguinetti Senior IEE Members, "Massive MIMO has unlimited Capacity ", 2017.

[4] K.P. Rajesh M. Mary Synthuja, "Enhanced Spectral Efficinecy for 5G Massive MIMO System", April 2019.

[5] Asif Ali, Iman Qureshi, Abdul latif Memon, and erum saba, "Spectral Efficiency of Massive MIMO Systems with Spatial Modulation", Vol. 9, 2018 .

[6] A. Wyner, "Shannon theoric approach to a gaussian cellular multiple access channel", pp. 1713-1727.

[7] Jehangir Arshad, "Spectral Efficiency Augmentation in Uplink Massive MIMO Systems by Increasung Transmit Power and unifrom Linear Array Gain ", September, 2020.

[8] A. Antonio Rouxinol Fragoso, "Impact of Massive MIMO Antennas on high Capacity 5G-NR Networks", Institute Superior Technico Vodafone, Portuga, 2020.

[9] Felipe A.P. de Figueiredo, "On the Applicaiton of Massive MIMO Systems to Machine Type Communication", Ghent University-imec, IDLab Department of IT, Belgium, 2020.

[10] T. L. Marzetta, "Massive MIMO: An introduction," 2015.

[11] Satya joshi, Sandrine Boumard, Marja Matin mikko, and Trevor Moore, "5G Enhanced Mobilebroadband Access netwokrs in crowded areas", Research and inoovation action, 2018.

[12] Nandana Rjatheva, "White Paper on Broadband Connectivity for 5G Network", arXv:2004.14247v1 [eess.SP], April 30, 2020.

[13] Hong Yang, Hein Q. Ngo, and Eric L. Larsson, " Multi-cell Massive MIMO System in LoS Propagation", arXiv :1808.04004v1[eess.SP], 12 August 2018.

[14] Tim Gagnon, "5G Mobile Technology, More devices, speed and mobility" , 2019.

[15] Thomas L. Marzetta, "Fundamentals of Massive MIMO ", United Kingdom : Cambrige University Press, 2016.

[16] H. Q. Ngo, "Massive MIMO: Fudamentals and systems Design", Division of communication systems, IEEE, 2015.

[17] Emil Bjornson, Jakob Hoydis, Luca Sanguineitti "Massive MIMO Networks: Spectral, Energy and Hardware Efficinecy", 2017.

[18] H. Q. Ngo, "Massive MIMO: Fundamentals and systems design", Linkoping University, 2015.

[19] A. A. L. Ashish Kumar, "4G Wireless Technology ", International Journal, 2013.

[20] G. Larsson, "Massive MIMO for Next generation Wireless Systems", IEEE Communication. Mag., , Feb. 2014.

[21] J. Hoydis, "Massive MIOM in the UL of cellular netwokrs", IEEE J. Sel. Areas Coomunication, Feb. 2013.

[22] Wei Xiang, "5G Mobile Coomunications", 2017..

[23] Emil Bjornson, "Optimal Design of Energy efficient Multi User MIMO Systems: is Massive MIMO the answer?", 2015.

[24] J. R. Hampton, "Introduction to MIMO Commuications", Cambridge university press, 2013.

[25] Jasmin, "Optimization of Spectral Efficiency in Massive MIMO TDD Systems wit Linear Processing", 2017.

[26] Emil Bjornson, "Massive MIMO for Maximal Spectral Efficiency: How many users and pilots should be allocated? ", 2016.

[27] A. Ghazanfari, "Power control for Multi-cell Massive MIMO ", Linkoping studies in science and techoloy Licentiate, 2019.

[28] S. Andrew, "What will be 5G?", IEEE J. Sel. Areas Commun., vol. Vol. 32, 2014.

[29] S. a. L. V. Boyd, "Convex Optimization ", Cambridge University Press, 2004.

[30] C. Y. Olakunle Elijah, "Mitigation of Pilot Contamination in Massive MIMO System for 5G", AN overview, IEEE, July, 2015.

[31] "An overview of Massive MIMO: benefits and challenges", IEEE J. Sel. Topics Singal Process, 2014.

[32] H. Q. Ngo, "Aspects of Favourable Propagation in Massive MIMO ", In proc. European singal processing conf. (EUSIPCO),IEEE, 2014.

[33] C. Paddington, "Power Allocation and user Selection in Multi-cell Multi-user Massive MIMO System", University of witwatersrand Johannesburg, south africa, 2017.

[34] R. C. a. R. Akl, "Massive MIMO Systems for 5G and Beyond Netwokrs-Overview Recent trends and chanllenges ", Department of computer science and engineering, Universty of North Texas, Denton, USA, May 2020.

[35] A. D. Aeron Wynner, "Shannon theoric approach to a gaussian cellular multiple access channel", IEEE Trans. Inf.